Accepted manuscript for Atmospheric Environment in 2009

Impacts of Asian dust storm associated with the stratosphere-to-troposphere transport in the spring of 2001 and 2002 on dust and tritium variations in Mount Wrangell ice core, Alaska

Teppei J. Yasunari[1] and Koji Yamazaki[2]

[1]Corresponding Author

[1]Research Institute for Humanity and Nature, Motoyama 457-4, Kamigamo, Kita-ku, Kyoto 603-8047, Japan. (teppei@chikyu.ac.jp)

[2]Graduate School of Environmental Science, Hokkaido University, Kita-10 Nishi-5, Sapporo 060-0810, Japan. (yamazaki@ees.hokudai.ac.jp)

Keywords: Asian dust, stratosphere-to-troposphere transport (STT), tritium, ice core, climate

Abstract: The relation of interannual connection between Asian dust outbreaks and stratosphere-to-troposphere transport (STT) in spring was suggested by the dust and tritium variations in the Mount Wrangell ice core, Alaska in Yasunari et al. (2007). However, these impacts on the ice core site in each event scale have not been investigated. Hence, the present paper focuses on the material transport and deposition processes for further understanding these impacts on the ice core. The variations in dust and tritium concentrations in spring in an ice core taken at Mt. Wrangell, Alaska are explained by meteorological analysis and simulation of trajectories associated with Asian dust outbreaks and STT. Material transport and deposition at Mt. Wrangell are examined in two contrasting years (2001 and 2002). Dust and tritium concentrations both reached peak values in the early spring of 2002, while the dust peak occurred in early spring and the tritium peak occurred in late spring in 2001. Six severe East Asian transpacific dust storms over this period are modeled by forward trajectory and meteorologically analyzed. It is found that 5 of 6 events contributed to the ice core record in Alaska. Stratospheric air is also transported to the ice core site in most cases. Tritium deposition is found to have been suppressed in the cases of the 2001 dust storms due to lack of snowfall at appropriate times. Taken the detailed transport and deposition processes after the severe dust storms with atmospheric circulations into account, we can well explain spring dust and tritium variations in the Mount Wrangell ice core.

1. Introduction

The impact of atmospheric dust on the global radiation budget is now reasonably well understood (Intergovernmental Panel on Climate Change (IPCC), 2007). The Gobi and Taklamakan deserts and other arid regions in East Asia are major sources of natural dust, referred to as Asian dust or *Kosa* in Japanese. Dust outbreaks in East Asia most commonly occur in spring, typically in association with the strong surface winds of cyclonic activity (Kurosaki and Mikami, 2003) and cold fronts (Sun et al., 2001; Hayasaki et al., 2006). The long-range transpacific transport of Asian dust has been discussed on many occasions, reaching Alaska, Canada, North America, and Greenland (Rahn et al., 1977; Biscaye et al., 1997; McKendry et al., 2001; Cahill, 2003; Darmenova et al., 2005; Zdanowicz et al., 2006; Yasunari et al., 2007). The widespread distribution of Asian dust in spring is therefore a crucial component of climate and material circulation.

On the other hand, it is known that the intrusion of stratospheric air into the troposphere (called, stratosphere-to-troposphere transport; STT) is an important meteorological phenomenon in terms of material exchange between the troposphere and stratosphere (Holton et al., 1995; Stohl et al., 2003). Stratospheric tracers such as tritium, ozone, and beryllium isotopes, move into the troposphere by STT (Gat et al., 2001; Monks, 2000; Zanis et al., 2003), which accompanies tropopause folding induced by strong cyclonic activities. Stratospheric tracers are often recorded as spring maxima. The STT also contributes to the ozone budget in the troposphere, although ozone is predominantly produced by photochemical production (Monks, 2000). As stratospheric materials such as ozone may affect the radiation balance and oxidation process in the troposphere, studies of STT using stratospheric tracers are considered essential in the investigation of material circulation and climate change.

The present study attempts to explain the spring variations in dust and tritium concentrations in an ice core drilled at the summit of Mt. Wrangell, Alaska (62°N; 144°W; 4100 m above sea level) (Shiraiwa et al., 2004), which is situated close to the Gulf of Alaska. This 50 m ice core was drilled in 2003, and the dust and tritium concentrations have previously been discussed in terms of contributions of Asian dust and related STT (Yasunari et al., 2007). In their study, a possible interannual connection between STT and Asian dust outbreaks in spring was found from the core flux data. However, the impacts on those relationships onto the ice core in each event scale have not been investigated.

In the present study, detailed transport and deposition processes relating to East Asian dust outbreaks are investigated by meteorological analysis and forward trajectory modeling with respect to the Mt Wrangell site. Six severe dust storms in the spring seasons of 2001 and 2002 are meteorologically analyzed and modeled, and the contributions to dust and tritium concentrations in the Mt. Wrangell ice core are determined.

2. Methods

The dynamic tropopause in the extratropics is commonly defined as having a potential vorticity (PV) of 2 potential vorticity units (PVU; 1 PVU = 10^{-6} K m^2 kg^{-1} s^{-1}) (e.g., Holton et al., 1995; Goering et al., 2001; Stohl et al., 2003). This definition is adopted in the present study. Data pertaining to geopotential height, temperature, ozone mixing ratio, relative humidity (RH), vertical and horizontal wind, PV at each pressure level, and wind at the 10 m surface, are taken as 6 h values from the 40 year reanalysis data set (ERA-40: 2.5º and 23-layer for horizontal and vertical resolutions, respectively) of the European Centre for Medium-Range Weather Forecasts (ECMWF) (Uppala et al., 2005). The potential temperature was calculated from temperature and pressure data, and surface pressure data were calculated from sea-level pressure, altitude, and geographical data.

The present study focuses on tritium, one of the stratospheric tracers, and its representation in the Mt. Wrangell ice core. As spatial information is unavailable for tritium, the spatial data for ozone from the ERA-40 data set were employed as a general description of the transport processes of stratospheric tracers. The ozone data in ERA-40 are relatively well reproduced over a large region of the stratosphere (Dethof and Holm, 2002). Although there remain some problems associated with the absolute values of the vertical structure of the analyzed ozone in the troposphere, the discussion in the present study considers the transport of ozone from the lower stratosphere to the upper troposphere and thus largely avoids these problems. At times of STT, the 2 PVU region is recognized as the tropopause, and air in the upper troposphere with increased ozone content along the 2 PVU line is identified as dry stratospheric air.

Forward trajectory analyses were performed for 6 severe dust storms in East Asia in the springs of 2001 and 2002. These dust storms occurred on April 6–7 and 8–9, 2001, and March 18(19)–22, 24–25, April 5(6)–9, and April 20(21)-24, 2002 (hereafter called, these dust storms as case-1, case-2, case-3, case-4, case-5, and case-6, respectively) (Liu et al., 2003; Shao and Wang, 2003; Shao et al., 2003; Zhou and Zhang, 2003; Darmenova et al., 2005; Sun et al., 2006; the Total Ozone Mapping Spectrometer (TOMS) data (for TOMS data, refer to the TOMS web site, http://toms.gsfc.nasa.gov/); simulation data of dust concentration by Spectral Radiation-Transport Model for Aerosol Species (SPRINTARS, Takemura et al., 2002) (for SPRINTARS data, refer to the website at http://sprintars.riam.kyushu-u.ac.jp/indexe.html).

The trajectory model was constructed based on the Lagrangian tracking method (Yamazaki, 1986). Horizontal and vertical wind data (three-dimensional wind data) from the ERA-40 data set for 2001 and 2002 were used for calculations. The wind data were interpolated linearly in the horizontal direction and by cubic spline interpolation in the vertical direction. The wind data were also interpolated linearly in time. The time step for the trajectory calculation is 20 min, and the output time interval is 2 h. Initial air parcels were set in initially defined boxes (Table 1), according to the initial central area of the cyclone and STT in each case. The initial area was divided horizontally into 900 bins (30×30) and vertically into 30 levels, extending from the lowermost stratosphere to the lower free troposphere. A total of 27,000 air particles were set in the initial box. The Wrangell Area was defined as the box in the region of 57–67°N latitude and 139–149°W longitude, extending over a pressure range of 500–650 hPa. Only the trajectories passing through the Wrangell Area are shown in the present analysis.

3. Results and discussion

3.1. Variations in dust and tritium in the Mount Wrangell ice core

Yasunari et al. (2007) presented an analysis of dust and tritium concentrations in the 50 m ice core drilled at the summit of Mt. Wrangell, Alaska. Fig. 1 shows a part of the analysis in which distinct dust and tritium peaks can be seen corresponding to the spring seasons of 2001 and 2002. The temporal resolutions of the dust and tritium analyses in the ice core are different due to the limited ice core samples and large amount of core sample by a factor of about 50 (as melt water) required for tritium analyses. The temporal resolution for the tritium analyses is approximately 1 month, while that for dust is 3–12 days. The 2001 dust peak in spring has been discussed previously (Yasunari et al., 2007) and has been attributed primarily to the "perfect" transpacific severe dust storm on April 6–7, 2001 (Darmenova et al., 2005). The 2002 dust peaks in spring have not been discussed.

Three large coarse-dust values accompanying elevated fine dust levels in the spring of 2002 can be seen in Fig. 1. In 2002, 4 severe dust storms were observed in East Asia, as referred from case-3 to case-6 (Table 2). No severe dust storms were recorded in May 2002 (Sun et al., 2006; Zhou and Zhang, 2003). The Aerosol Index intensity data for the 4 severe dust storms present in the TOMS data indicate transpacific transport and strong intensities for all 4 events. Hence, these 4 dust storms from case-3 to case-6 were investigated in terms of the impacts on the ice core dust and tritium data.

The spring maxima of dust and tritium in 2001 are located at different depths in the ice core, whereas the spring maximum of dust occurs within the enhanced tritium zone in the core depth interval corresponding to 2002 (Fig. 1). In the 2002 period, the tritium level in late spring (b2) is lower than that in early spring (a2), while the opposite variation is observed in 2001 (b1 > a1). The spring tritium peaks are attributable to STT events, which may be associated with not only Asian dust storms but also eddy development in other regions such as the North Pacific Ocean. The contribution of STT associated with other events cannot be excluded because STT also occurs in the North Pacific Ocean (Sprenger and Wernli, 2003). However, as a first step, present study mainly focuses on the impacts of transport and deposition processes of Asian dust and stratospheric tracers associated with Asian dust STT on the variations of dust and tritium in the Mount Wrangell ice core.

3.2. Simultaneous dust storm and STT events in April 2001

The “perfect” severe dust storm (case-1 in Table 2) was detected by several satellite sensors as a dust cloud over the North Pacific (Darmenova et al., 2005). This event has been visualized on the basis of Moderate Resolution Imaging Spectroradiometer (MODIS) and TOMS data by the Scientific Visualization Studio (SVS; http://svs.gsfc.nasa.gov/vis/a000000/a002800/a002860/). Dust associated with this event was detected at a number of distant locations at later dates, including the Gulf of Alaska on April 12–13, 2001 (see TOMS and SVS data; Darmenova et al., 2005).

Coarse dusts were observed at Adak Island, one of the southernmost Aleutian Islands of Alaska, on 13 April 2001 (Cahill, 2003), higher altitudes in the St. Elias Mountains, Yukon Territory, Canada (Zdanowicz et al., 2006), and an ice core site of Mount Wrangell, Alaska (Yasunari et al., 2007).

Fig. 2a illustrates atmospheric circulation field associated with development of the dust storm. At 12:00 coordinated universal time (UTC) on April 6, 2001, a cyclone emerged in the area extending from approximately 40–50°N to 100–120°E. Stratospheric ozone advection into the troposphere with strong downward wind along the 2 PVU tropopause line was detected at this time (Fig. 2b and S1: All the supplemental figures are shown with symbol S, hereafter), extending from the northwest to the southeast of the area. The dust storm broke out in this area on April 6 in association with strong surface winds (Darmenova et al., 2005). Stratospheric air moved into the troposphere along the 310 K isentropic surface with strong downward wind (The arrow in Fig. 2b and S1b).

Fig. 3 shows the corresponding 8 day forward trajectories, starting from the dust storm area at 250–700 hPa in East Asia. The trajectories in the lower free troposphere passed near the boundary layer over the eastern side of the Eurasian continent during the first 2 days, consistent with the migration of the dust cloud from East Asia to the North Pacific Ocean region seen in the TOMS and SVS data. The trajectories also show that the air mass from the lower troposphere had migrated to the vicinity of the summit of Mt. Wrangell by April 14. This trajectory analysis clarifies the dust transport associated with the April 6 dust storm, and confirms that the coarse dust peak and accompanying elevation in fine dust seen in the ice core can be attributed predominantly to this severe dust storm (Fig. 1). The results of the present study, and those reported by Zdanowicz et al. (2006) and Yasunari et al. (2007), imply that the long-range transport of coarse Asian dust in spring can be regarded as a common phenomenon at higher altitude in the

North Pacific region.

On April 6, parts of the stratospheric air parcels in the initial area underwent rapid movement into the lower free troposphere (Figs. 2b and S1b) over a period of 1 day associated with the development of the cyclone (Fig. 2a). The trajectories describing this movement can be seen in Fig. 3 as a migration on day 1 (a2, yellow) and corresponding to the trajectory parts in red in Fig. 3(b2). The northward-traveling branches of the 400–250 hPa air mass (near 60°N) in Fig. 3(b1) largely remained in the upper troposphere during April 6-9 From 12:00 UTC, April 9, to 12:00 UTC, April 11, the air mass in the upper troposphere was transported rapidly to the middle troposphere, as seen from the corresponding downstream trajectories in Fig. 3(a2, yellowish green and purple). We checked the atmospheric circulation pattern on April 11 in the fields of geopotential height and horizontal and vertical wind at that time (Fig. 4). The pattern clearly showed the developing cyclone near the Alaska Peninsula, which intensified the downward motion of the air mass at the southwest end of the trough (Fig. 4). This cyclone effectively conveyed the air mass from the upper troposphere to the middle troposphere, likely also involving in other stratospheric-origin material on April 9 (Fig. S2) (i.e., STT due to other processes). The air masses originating in the North Pacific stratosphere, associated with both the Asian dust storm and this developing cyclone, thus met and mixed near 180°E. The majority of the combined air mass then passed the Mt. Wrangell Area on April 12. We can clearly understand stratospheric material impacts on the ice core site due to STT with Asian dust storm and other STT in the North Pacific region from an animation movie of ozone at 300 hPa (see supplementary movie). A fraction of the air mass returned to the summit region of Mt. Wrangell from the direction of the Arctic on April 14, as indicated by the upper trajectories at less than 400 hPa in Fig. 3(a2, red) and the narrow returning trajectories in Figs. 3(a1, b1: red). The main dust cloud reached the Wrangell Area on April 14, 2001. The important feature to note is the simultaneity of the dust storm outbreak and the STT, and the dissimilarity between the paths and velocities (2 day lag) of the dust cloud and the stratospheric air masses.

Zdanowicz et al. (2006) reported that Asian dust fell in the St. Elias Mountains in association with snowfall, with assumed deposition dates of April 11–19, 2001. Mount Logan, at which the measurements reported in Zdanowicz et al. (2006) were carried out is located approximately 240 km from Mt. Wrangell. Synoptic-scale cyclones may impact on these mountains at the same time. The results of Zdanowicz et al. (2006) are therefore considered comparable to those in the present study.

Fig. 5 shows the vertical variation in RH and ozone from the ERA-40 data set for the region above the Mt. Wrangell ice core site at the time of dust and stratospheric tracer transport. The ice core site (4100 m above sea level) roughly corresponds to the 600 hPa surface. The trajectories of upper transport including the stratospheric air mass (Fig. 3(b2, red)) reached the Mt. Wrangell area on April 12, 2001 (orange/blue boundary in Fig. 3(a1)), at which time a zone of relatively dry air with increased ozone was present above the summit. The increase in ozone is attributable to transport of the stratospheric-origin air mass mixed with Asian dust-related STT on April 6–7 and STT due to other processes on April 9–11 in the vicinity of 180°E (Fig. S2). After April 12, the air of stratospheric origin turned clockwise by 360° (Fig. 3(a1)), and the moister dust cloud was transported to Mt. Wrangell by April 14 after passing through the lower free troposphere above the North Pacific Ocean. Most of the upper trajectories reached Canada via the Arctic Ocean, and the air trajectories in the upper troposphere returned to the vicinity of Mt. Wrangell on April 13-14. The dry stratospheric-origin air remained in place above 400 hPa (Figs 3(a2, red above 400 hPa) and 5), while high-humidity air was predominant below 400 hPa on April 13–15. These conditions are not favorable for tritium deposition with snowfall because tritium mainly exists as tritiated water vapor in the atmosphere (Gat et al., 2001) and prefers wet deposition (Yasunari et al., 2007).

As the stratospheric air in this period stayed above 400 hPa and remained dry, snow deposition would mainly have occurred below 400 hPa, entraining dust from levels below 400 hPa. The major stratosphere-origin trajectories passed the Mt. Wrangell area on April 12. On that day, relatively dry air with increased ozone was dominant above the ice core site, and significant snowfall would have been unlikely. Tritium deposition associated with the April 6 Asian dust storm may therefore be considerably lower than in cases involving persistent snowfall, causing the tritium concentration in the early spring 2001 interval of the ice core (Fig. 1(a1 peak)) to be lower than expected. However, the tritium concentration for this interval in the early spring 2001 is still considerably higher than the background level.

A case-2 dust storm broke out in the same region on April 8–9, 2001 (Fig. S3, Table 2). Tropopause folding and STT was also identified in the same region as for the April 6 dust storm (Figs. S3c and S3d). The 6 day forward trajectories from 6:00 UTC on April 9 to 6:00 UTC on April 15 revealed that only a small number of trajectories extending from the dust storm to the Mt. Wrangell area included air mass contributions from the lower troposphere (Fig. S4). The result implies that dust contribution to the Wrangell Area in this case is expected, whereas the stratospheric air contribution is expected to be less.

3.3. Simultaneous dust storm and STT events in March and April 2002

Fig. 6a illustrates the development of the case-3 dust storm (Table 2). A deepening cyclone on the southeast side of Lake Baikal caused the dust outbreak in the Gobi desert region (Sun et al., 2006). A deep STT occurred accompanying strong downward wind on the south side of the cyclone (Figs. 6b, S5a, and S5b). The ozone intrusion from the stratosphere corresponds well with the strong vertical wind variation. Tritium may also have intruded into the troposphere in this region at this time. The STT in this case was the deepest of those examined in the present study in terms of downward wind velocity and ozone descent to the 750 hPa layer.

The trajectories from the lower troposphere and lower stratosphere were well mixed vertically, and did not branch off on the transport pathways to Mt. Wrangell (Fig. 7). This is an important difference from the case-1 dust storm in 2001 (see Figs. 3 and 7).

The dust and stratospheric air reached the Mt. Wrangell Area after March 26 (Fig. 7(a1, a2)). The relative humidity at the summit of Mt. Wrangell on March 26–28 exceeded 80%, indicating that snowfall is likely to have occurred throughout this period (Fig. 8a). As the air mass transported from the lower troposphere is likely to have encountered moist air during passage over the North Pacific Ocean (Fig. 7(b1, b2: dark blue), 700–600 hPa trajectories), the arrival of the air mass at Mt. Wrangell coincides with the increase in RH at the ice core site (Figs. 7 and 8a). The ozone volume mixing ratio at the ice core site on March 26 was higher than 0.12 ppmv, to which stratospheric air from East Asia is considered to contribute. Hence, tritium is also likely to have been transported and deposited efficiently by snowfall at this time.

The dust storm on March 18(19)–22 was followed by another on March 24-25 (Fig. S6; case-4 in Table 2). Ozone intrusions were observed accompanying tropopause folding at 52.5°N (see the arrows in Figs. S6c and S6d), although the intrusion was relatively weak. Descending air is distinctly observable at 42.5°N, 100°E (Fig. S7b, 400–250 hPa trajectories in red). The origin of this descending air is the upper troposphere, not the stratosphere, owing to the very flat structure of the tropopause in this region at 250 hPa (not shown). The descending area was out of the tropopause line of 2 PVU, corresponding to the troposphere (Fig. S6b). Only a few trajectories from the lower troposphere will have contributed to the ice core record at Mt. Wrangell in this case. (Fig. S7). The trajectories extending from the lower troposphere originated not in the dust outbreak area, but those passed through the dust cloud in the vicinity of Hokkaido, Japan (Figs. S7(a1,b1; see also TOMS data)). Hence, although fewer trajectories arrived at Mt. Wrangell than in the case-3, case-4 dust storm is likely to be represented in the ice core dust record at Mt. Wrangell. However, the contribution of stratospheric air (i.e., tritium) associated with Asian dust-related STT is not expected in the Wrangell Area for this event because red trajectories from the upper troposphere did not indicate STT (Figs. S6b and S7). Although ozone above 500 hPa increased from March 30 to April 1 associated with low RH (Fig. 8a), this air mass is due to STT from Arctic stratosphere (not shown). The RH on the relevant days was also very low at the ice core site, and tritium deposition by snowfall is not expected. Hence, the tritium contributions of both Asian dust-related STT and STT due to other processes are likely to be very small at the ice core site for this event. It is likely that only Asian dust contributes to the ice core in this case.

In the case-5 dust storm (Table 2), the aerosol index on its transpacific transport was higher (see TOMS data). The development of this dust storm is illustrated in Fig. S8. A cyclone had developing on the southeast side of Lake Baikal on April 6, similar to the location of the cyclone associated with the case-1 dust storm. The ozone advection pattern from northwest to southeast is also very similar (Figs. S1a and S8b). However, the vertical structure indicates that the air mass intrusion due to Asian dust-related STT was much deeper than in the April 6–7, 2001 event. Fig. S9 shows the trajectory calculations from 0:00 UTC on April 6, 2002 in the region of the developing cyclone. The air masses reached the Mt. Wrangell Area on April 14-15, 2002, and were well mixed vertically during transport (Figs, S9(a2, b2)). The relative humidity on April 14 was very high in the summit region of Mt. Wrangell, and highly saturated layers were developing toward the upper troposphere (Fig. 8b). Dust from this storm and tritium due to Asian dust-related STT are therefore expected to have been efficiently deposited by snowfall at the ice core site on April 14, 2002.

In the case-6 dust storm case, a cyclone was developing on the southeast side of Lake Baikal as same as the other cases but it was weakest (Fig. S10a). Associated STT was not seen (Figs. S10c and S10d). Actually, the number of station which observed dust storm was much less than that of case-1, case-3, and case-5 (Zhou and Zhang, 2003; Sun et al., 2006). Additionally, the dust storm on that day mainly occurred at the lower latitude than 45˚N, which was verified in the TOMS and SPRINTARS data. The calculated trajectories showed that only the air mass of higher than 45˚N was coming to the Mount Wrangell area (Fig. S11). Hence, dust and tritium contributions due to this dust storm to the Wrangell ice core are considered to be less and that is why the dust concentration in the ice core did not increase so much.

3.4. Dating of dust peaks in 2002

The present models suggest that Asian dust deposition due to case-3, case-4, and case-5 events occurred on March 26–28, April 1 (dust only), and April 14–15, corresponding to temporal separations of approximately 4–6 days and 13–14 days, respectively. For the period of interest, the temporal resolution of ice core samples is approximately 6 days (65 samples from the late spring of 2001 to the late spring of 2002). The first and second of the coarse dust peaks in the spring of 2002 are adjacent in the ice record, corresponding to an interval within 6 days, which is consistent with the model results. The interval between the second and third dust peaks is marked by 3 samples, corresponding to an interval of 12–18 days, which is also consistent with the modeled interval of 13–14 days. Therefore, the temporal intervals of ice core were well explained by the actual transport intervals.

3.5 Characteristics of tritium deposition

As the half-life of tritium is 12.32 years (Lucas and Unterweger, 2000), the tritium decay from spring 2001 to spring 2002 (one year) is approximately 5%. However, even taking the decay of tritium into account, the tritium concentration in the early spring of 2002 (Fig. 1, a2) is much larger than that in the early spring of 2001 (Fig. 1, a1), which was obtained from the ice core (Yasunari et al., 2007). The perfect transport of Asian dust and tritium, followed by efficient snowfall deposition, is considered to be responsible for the high tritium concentration at the a2 peak in 2002. As demonstrated in this present, accurate modeling of the transport and investigating deposition processes by means of meteorological analysis satisfactorily explains the dust and tritium variation in the Mt. Wrangell ice record for spring seasons of 2001 and 2002.

In some cases, such as the 2001 case, stratospheric air from the Asian dust region was not effectively deposited at the ice core site. However, the stratospheric air intrusion to the troposphere enhances the tritium level in the upper troposphere. It is also natural that the Alaskan ice core is more sensitive to STT near the ice core site, such as in the North Pacific, than that in the Asian dust region due to cyclonic activities. Future studies require the assessment for those relationships among East Asia and the North Pacific. This may explain the interannual correlation between tritium and dust reported by Yasunari et al. (2007).

4. Conclusion

Distinct differences in the transport and deposition processes were found for the spring Asian dust storms of 2001 and 2002. In 5 of 6 cases of severe Asian dust storms, the dust outbreak occurred simultaneously with STT in the dust storm area, indicating that severe cyclone development is very important for causing Asian dust outbreak with

STT. The variations of dust and tritium concentrations in the spring 2001 and 2002 in the ice core were well explained by the differences of transport and deposition patterns of dust and related STT after we investigated 6 severe dust storms in East Asia. These results also well reflect that dust deposits by both dry and snow (wet) depositions but tritium deposition is mainly occurred by snow (wet) deposition. The present results will be helpful for interpreting the records of ice cores drilled at mountain glaciers in the North Pacific region, and also in understanding the interaction of the Asian dust storm and STT from East Asia with the North Pacific Ocean and hence the North Pacific climate system. In future studies, it is important for examining in detail the relationship between STT with and without Asian dust storm because we found examples of its connections from animation movies of ozone and 2 PVU line in April 2001 (see supplementary movie). It will more helpful for understanding the interannual relationship between dust and tritium by Yasunari et al. (2007). Further studies on spring cyclonic activities in the North Pacific region are key to investigate the Asian dust outbreak, STT, and snowfall at mountain glaciers in the North Pacific region. It finally contributes to assess spring material circulations from the stratosphere to the troposphere.

Acknowledgements

We appreciate helpful comments from two anonymous reviewers. All the ERA-40 except for the ozone data and PV data were provided from the data server, blade, of the Course in Atmosphere-Ocean & Climate Dynamics of the Graduate School of Environmental Science, Hokkaido University, Japan. Kazuhiro Oshima of the Graduate School of Environmental Science, Hokkaido University, Japan is gratefully acknowledged for assistance with data preparation. The ozone and PV data in ERA-40 used here were also directly obtained from ECMWF. The ERA-40 data were produced

by ECMWF. Figures were prepared using the Grid Analysis and Display System (GrADS) and the GFD DENNOU Library.

References

Biscaye, P. E., F. E. Grousset, M. Revel, S. VanderGaast, G. A. Zielinski, A. Vaars, and G. Kukla, 1997, Asian provenance of glacial dust (stage 2) in the Greenland Ice Sheet Project 2 Ice Core, Summit, Greenland, *J. Geophys. Res.*, *102*(C12), 26,765–26,781.

Cahill, C. F., 2003, Asian aerosol transport to Alaska during ACE-Asia, *J. Geophys. Res.*, *108*(D23), 8664, doi:10.1029/2002JD003271.

Dethof, A., and E. Holm, 2002, Ozone in ERA40: 1991-1996, *ECMWF Tech. Memo*., **377**., pp.37.

Darmenova, K., I. N. Sokolik, and A. Darmenov, 2005, Characterization of east Asian dust outbreaks in the spring of 2001 using ground-based and satellite data, *J. Geophys. Res.*, *110*(D2), D02204, doi:10.1029/2004JD004842.

Gat, J. R., W. G. Mook, and H. A. J. Meijer, 2001, Tritium in the atmosphere, in *Atmospheric Water: Environmental Isotopes in the Hydrological Cycle Principles and Applications*, vol. II, edited by W. G. Mook, pp. 63–74, UNESCO/IAEA Series, Paris. (Available at: http://www.iaea.org/programmes/ripc/ih/volumes/volumes.htm.)

Goering, M. A., W. A. Gallus, M. A. Olsen, and J. L. Stanford, 2001, Role of stratospheric air in a severe weather event: Analysis of potential vorticity and total ozone, *J. Geophys. Res.*, *106*(D11), 11,813–11,823.

Hayasaki, M., S. Sugata, and H. L. Tanaka, 2006, Interannual variation of cold frontal activity in spring in Mongolia, *J. Meteorol. Soc. Jpn.*, *84*(3), 463–475.

Holton, J. R., P. H. Haynes, M. E. Mcintyre, A. R. Douglass, R. B. Rood, and L. Pfister, 1995, Stratosphere-troposphere exchange, *Rev. Geophys.*, *33*(4), 403–439.

IPCC, 2007: Summary for Policymakers. In: *Climate Change 2007: The Physical Science Basis. Contribution of Working Group I to the Fourth Assessment Report of the Intergovernmental Panel on Climate Change*, edited by Solomon, S., D. Qin, M. Manning, Z. Chen, M. Marquis, K.B. Averyt, M.Tignor and H.L. Miller, Cambridge University Press, Cambridge, UK and New York, NY, USA.

Kurosaki, Y., and M. Mikami, 2003, Recent frequent dust events and their relation to surface wind in East Asia, *Geophys. Res. Lett.*, *30*(14), 1736, doi:10.1029/2003GL017261.

Liu, M., D. L. Westphal, S. G. Wang, A. Shimizu, N. Sugimoto, J. Zhou, and Y. Chen, 2003, A high-resolution numerical study of the Asian dust storms of April 2001, *J. Geophys. Res.*, *108*(D23), 8563, doi:10.1029/2002JD003178.

Lucas, L. L., and M. P. Unterweger, 2000, Comprehensive review and critical evaluation of the half-life of tritium, *J. Res. Natl. Stand. Technol.*, *105*(4), 541–549.

McKendry, I. G., J. P. Hacker, R. Stull, S. Sakiyama, D. Mignacca, and K. Reid, 2001, Long-range transport of Asian dust to the Lower Fraser Valley, British Columbia, Canada, *J. Geophys. Res.*, *106*(D16), 18,361–18,370.

Monks, P. S., 2000, A review of the observations and origins of the spring ozone maximum, *Atmos. Environ.*, *34*(21), 3545–3561.

Rahn, K. A., R. D. Borys, and G. E. Shaw, 1977, Asian source of Arctic haze bands, *Nature*, *268*, 713–715.

Shao, Y. P., and J. J. Wang, 2003, A climatology of Northeast Asian dust events, *Meteorol. Z.*, *12*(4), 187–196.

Shao, Y. P., *et al.*, 2003, Northeast Asian dust storms: Real-time numerical prediction and validation, *J. Geophys. Res.*, *108*(D22), 4691, doi:10.1029/2003JD003667.

Shiraiwa, T., S. Kanamori, C. S. Benson, D. Solie, and Y. D. Muravyev, 2004, Shallow ice-core drilling at Mount Wrangell, Alaska, *Bull. Glaciol. Res.*, *21*, 71–77.

Sprenger, M., and H. Wernli, 2003, A northern hemispheric climatology of cross-tropopause exchange for the ERA15 time period (1979-1993), *J. Geophys. Res.*, *108*(D12), 8521, doi:8510.1029/2002JD002636.

Stohl, A., et al., 2003, Stratosphere-troposphere exchange: A review, and what we have learned from STACCATO, *J. Geophys. Res.*, *108*(D12), 8516, doi:10.1029/2002JD002490.

Sun, J. M., M. Y. Zhang, and T. S. Liu (2001), Spatial and temporal characteristics of dust storms in China and its surrounding regions, 1960-1999: Relations to source area and climate, *J. Geophys. Res.*, *106*(D10), 10,325–10,333.

Sun, J. H., et al., 2006, An integrated dust storm prediction system suitable for East Asia and its simulation results, *Glob. Planet. Change*, *52*(1–4), 71–87.

Takemura, T. , T. Nakajima, O. Dubovik, B. N. Holben, and S. Kinne, 2002, Single-scattering albedo and radiative forcing of various aerosol species with a global three-dimensional model., *J. Clim.*, 15, 333-352.

Uppala, S. M., et al., 2005, The ERA-40 re-analysis, *Q. J. R. Meteorol. Soc.*, *131*, 2961–3012.

Yamazaki, K., 1986, Preliminary calculation of trajectory analysis in the lower stratosphere of the southern-hemisphere, *Geophys. Res. Lett.*, *13*(12), 1312–1315.

Yasunari, T. J., T. Shiraiwa, S. Kanamori, Y. Fujii, M. Igarashi, K. Yamazaki, C. S. Benson, and T. Hondoh, 2007, Intra-annual variations in atmospheric dust and tritium in the North Pacific region detected from an ice core from Mount Wrangell, Alaska, *J. Geophys. Res.*, *112*, D10208, doi:10.1029/2006JD008121.

Zanis, P., et al., 2003, An estimate of the impact of stratosphere-to-troposphere transport (STT) on the lower free tropospheric ozone over the Alps using Be-10 and Be-7 measurements, *J. Geophys. Res.*, *108*(D12), 8520, doi:10.1029/2002JD002604.

Zhou, Z. J., and G. C. Zhang, 2003, Typical severe dust storms in northern China during 1954—2002, *Chin. Sci. Bull.*, *48*(21): 2366–2370.

Zdanowicz, C., G. Hall, J. Vaive, Y. Amelin, J. Percival, I. Girard, P. Biscaye, and A. Bory, 2006, Asian dustfall in the St. Elias Mountains, Yukon, Canada, *Geochim. Cosmochim. Acta*, *70*(14), 3493–3507.

Figure captions

Fig. 1. Recorded ice core data corresponding to 2000 to 2002, showing fine dust (red solid line; left scale; size range, 0.52–1.00 μm), coarse dust (gray solid line; left scale; size range, 1.00–8.00 μm), and tritium concentration (blue solid line; right scale). Figure is reproduced from Yasunari et al., 2007. The vertical lines denote the relative center positions of early spring (orange), late spring (yellowish green), summer (yellow), autumn (violet), and winter (sky blue).

Fig. 2. Meteorological conditions for Asian dust storm at 12:00 UTC on April 6, 2001. (a) Geopotential height at 850 hPa (shaded contour; unit: m) and surface wind at 10 m (green vector; unit: m s^{-1}). (b) Ozone volume mixing ratio (shaded contour; unit: ppmv), 2 PVU tropopause line (blue solid line), potential temperature (PT; white solid line; unit: K), and vertical p-velocity (omega; black contour; only downward components are plotted; unit: Pa s^{-1}), at the 107.5°E line for the cross-section between latitude and pressure level (<500 hPa). Data grid is interpolated to a finer grid by cubic interpolation. Black solid line in Fig. 2a corresponds to the lines at 107.5°E. Black arrow in Fig. 2b denotes the place at which STT is occurring.

Fig. 3. Recorded trajectories from initial area of the Asian dust storm at 12:00 UTC on April 6, 2001 to the Wrangell Area. (a1,a2) Trajectories by day (each color denotes transport for 1 day: in order of yellow, blue, sky-blue, green, purple, orange, dark blue, and red). (b1,b2) Trajectories by initial pressure level of air mass (700–600 hPa, blue; 600–400 hPa, green; 400–250 hPa, red).

Fig. 4. Geopotential height (shaded contour; unit: m), horizontal wind (gray vector; unit: m s^{-1}), and vertical p-velocity (omega; green contour; unit: Pa s^{-1}) at 600 hPa pressure

level, 0:00 UTC on April 11, 2001. Data grid is interpolated to a finer grid by cubic interpolation.

Fig. 5. Ozone volume mixing ratio (white contour; unit: ppmv) and RH (shaded contour; unit: %) at Mt. Wrangell (nearest grid point in ERA40 data is 62.5°N, 145°W) from 12:00 UTC on April 6 to 0:00 UTC on April 17, 2001. Summit is at roughly the 600 hPa level. Data grid is interpolated to a finer grid by cubic interpolation.

Fig. 6. Similar to Figure 2 but for the Asian dust storm at 6:00 UTC on 20 March 2002. (b) is at the 115°E line for the cross section between latitude and pressure level (<775 hPa). Black solid line in Fig. 6a corresponds to the lines at 115°E. Gray arrow in Fig. 6b denotes the place at which STT is occurring.

Fig. 7. Similar to Figure 3 but for the Asian dust storm at 6:00 UTC on 20 March 2002.

Fig. 8. Ozone volume mixing ratio (white contour; unit: ppmv) and relative humidity (shaded contour; unit: %) at Mount Wrangell (nearest grid point in ERA-40 data is 62.5°N, 145°W) (a) from 6:00 UTC on 20 March 2002 to 6:00 UTC on 1 April 2002 and (b) from 0:00 UTC on 6 April 2002 to 0:00 UTC on 15 April 2002. The summit of Mount Wrangell is roughly at the 600-hPa level. The data grid is interpolated to a finer grid using cubic interpolation.

Table 1. Initial boxes for forward trajectory calculations

Time set	Longitude	Latitude	Pressure (hPa)	Calculation term (days)
12:00 UTC, April 6, 2001	100–120ºE	40–50ºN	700–250	8
6:00 UTC, April 9, 2001	100–120ºE	35–50ºN	700–250	6
6:00 UTC, March 20, 2002	105–120ºE	35–48ºN	700–250	8
6:00 UTC, March 24, 2002	100–120ºE	42.5–52.5ºN	700–250	8
0:00 UTC, April 6, 2002	105–115ºE	42–48ºN	700–250	9
12:00 UTC, April 20, 2002	105–130ºE	40–50ºN	700–250	5

Table 2. Summary of picked up dust storms in the spring of 2001 and 2002 and the estimated arrival date of these dusts to the Wrangell Area

Dust storm No.	Date of severe dust outbreak	Arrival date of dust over Mt. Wrangell and date of dust layer
case-1	6-7 April 2001	14 April 2001
case-2	8-9 April 2001	15 April 2001
case-3	18(19)-22 March 2002	26-28 March 2002
case-4	24-25 March 2002	1 April 2002
case-5	5(6)-9 April 2002	14-15 April 2002
case-6	20(21)-24 April 2002	not arrived

Figure 1

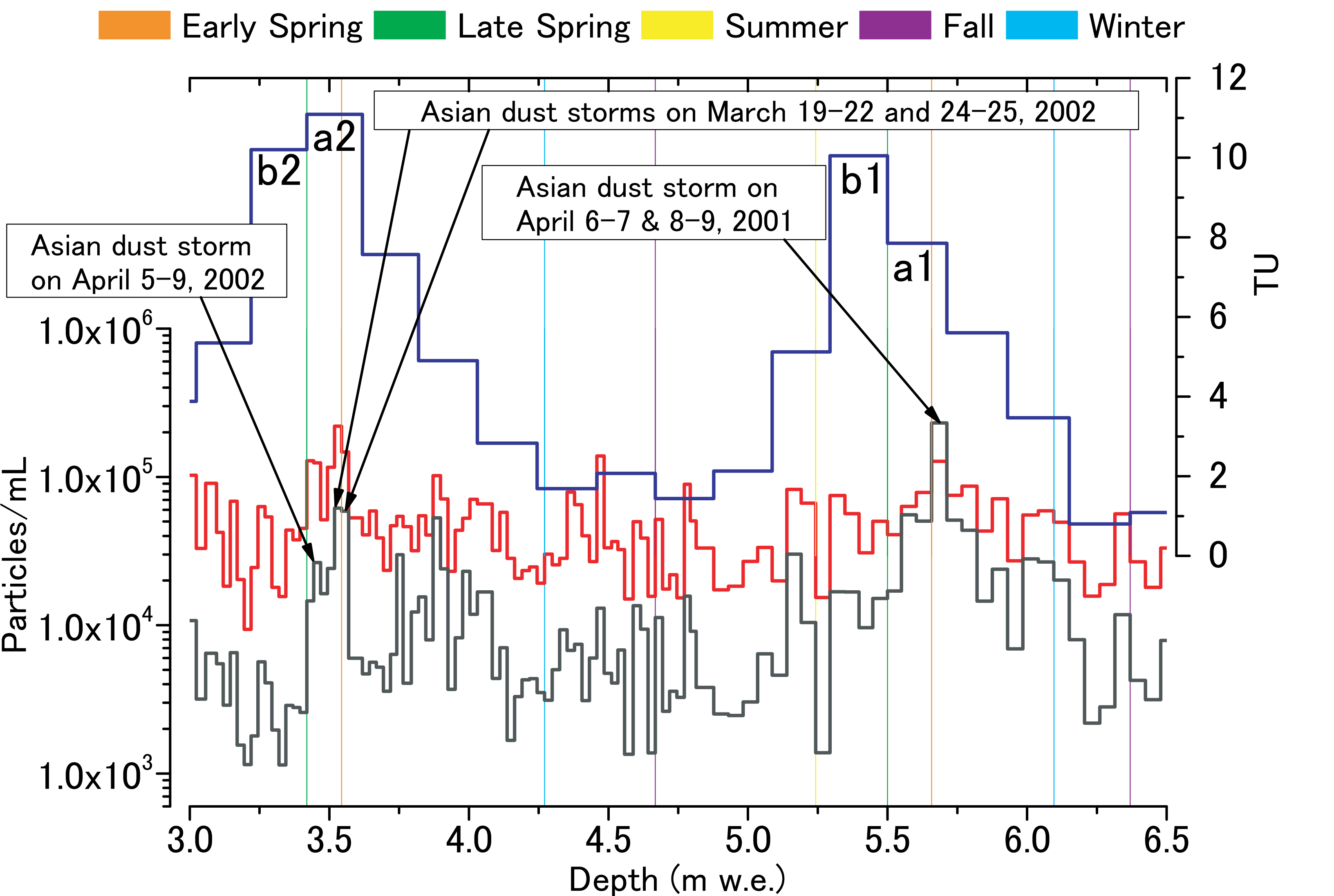

Early Spring
Late Spring
Summer
Fall
Winter
Asian dust storms on March 19-22 and 24-25, 2002
Asian dust storm on April 6-7 & 8-9, 2001
Asian dust storm on April 5-9, 2002
a2
b2
b1
a1
Particles/mL
1.0x10^6
1.0x10^5
1.0x10^4
1.0x10^3
TU
12
10
8
6
4
2
0
3.0
3.5
4.0
4.5
5.0
5.5
6.0
6.5
Depth (m w.e.)

Figure 2

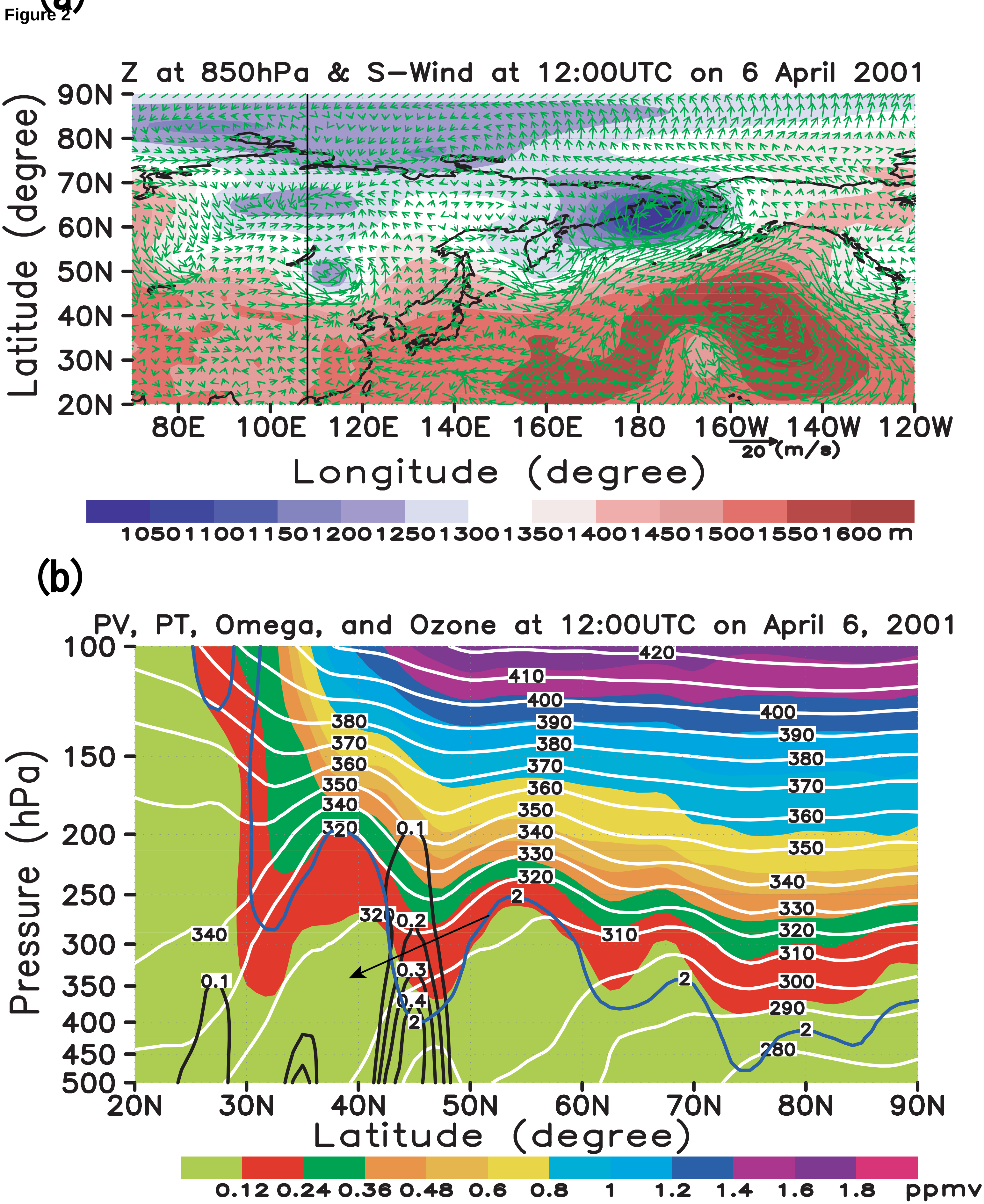
(a)
Z at 850hPa & S-Wind at 12:00UTC on 6 April 2001
Latitude (degree)
90N
80N
70N
60N
50N
40N
30N
20N
80E 100E 120E 140E 160E 180 160W 140W 120W
20 (m/s)
Longitude (degree)
1050 1100 1150 1200 1250 1300 1350 1400 1450 1500 1550 1600 m
(b)
PV, PT, Omega, and Ozone at 12:00UTC on April 6, 2001
Pressure (hPa)
100
150
200
250
300
350
400
450
500
20N 30N 40N 50N 60N 70N 80N 90N
Latitude (degree)
0.12 0.24 0.36 0.48 0.6 0.8 1 1.2 1.4 1.6 1.8 ppmv

Figure 3
Click here to download high resolution image

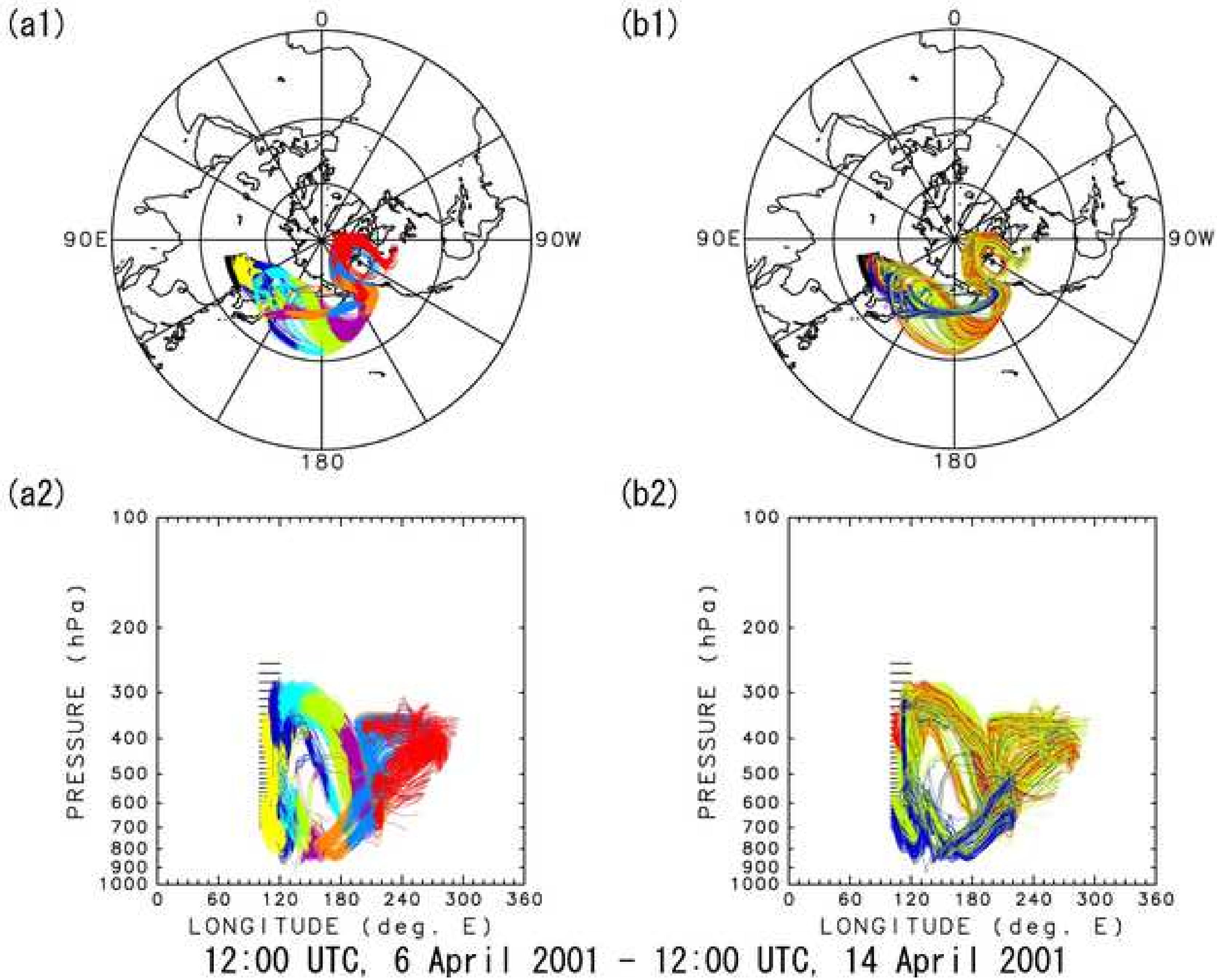

Figure 4

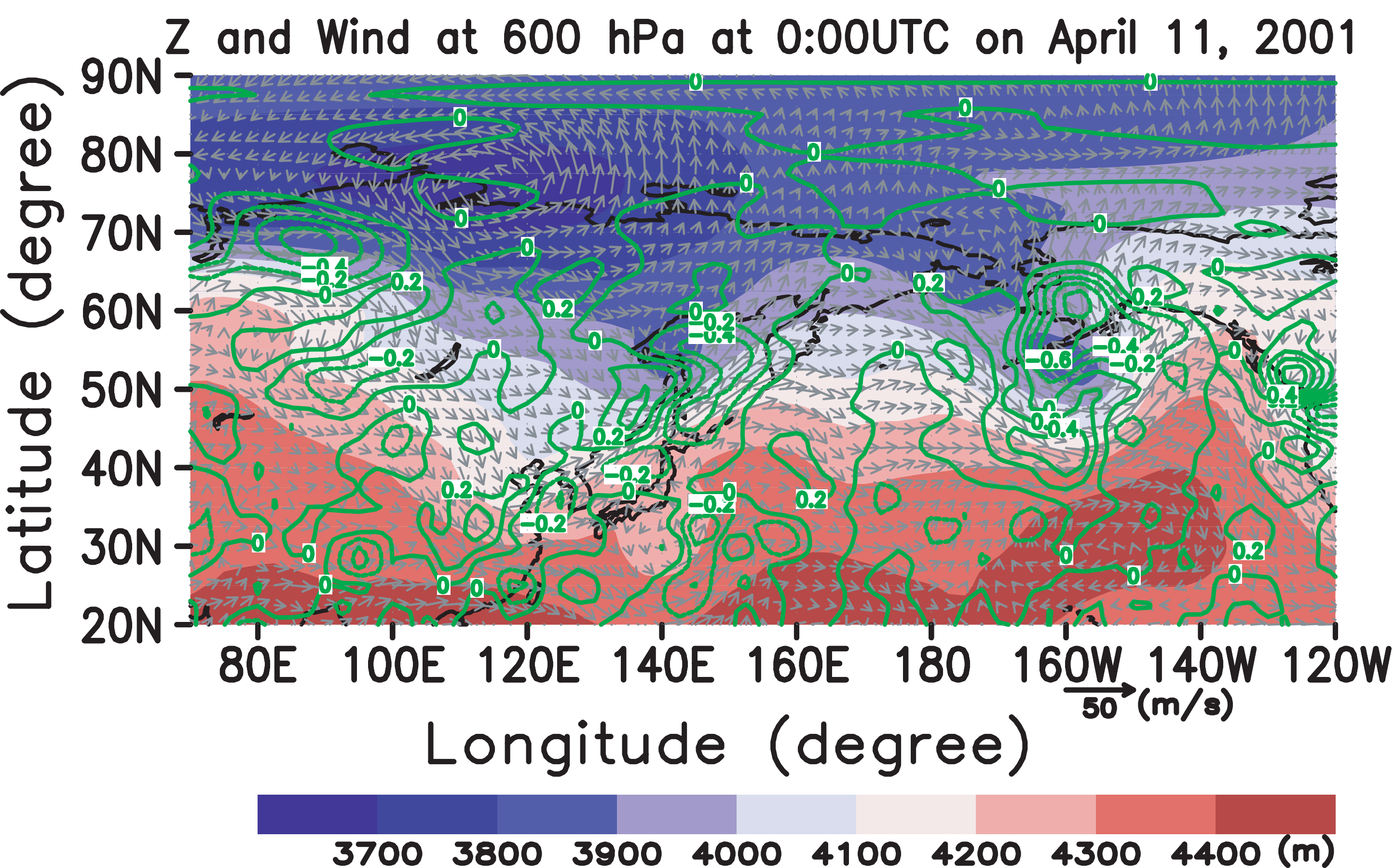

Z and Wind at 600 hPa at 0:00UTC on April 11, 2001
Latitude (degree)
90N
80N
70N
60N
50N
40N
30N
20N
80E
100E
120E
140E
160E
180
160W
140W
120W
50 (m/s)
Longitude (degree)
3700
3800
3900
4000
4100
4200
4300
4400
(m)

Figure 5

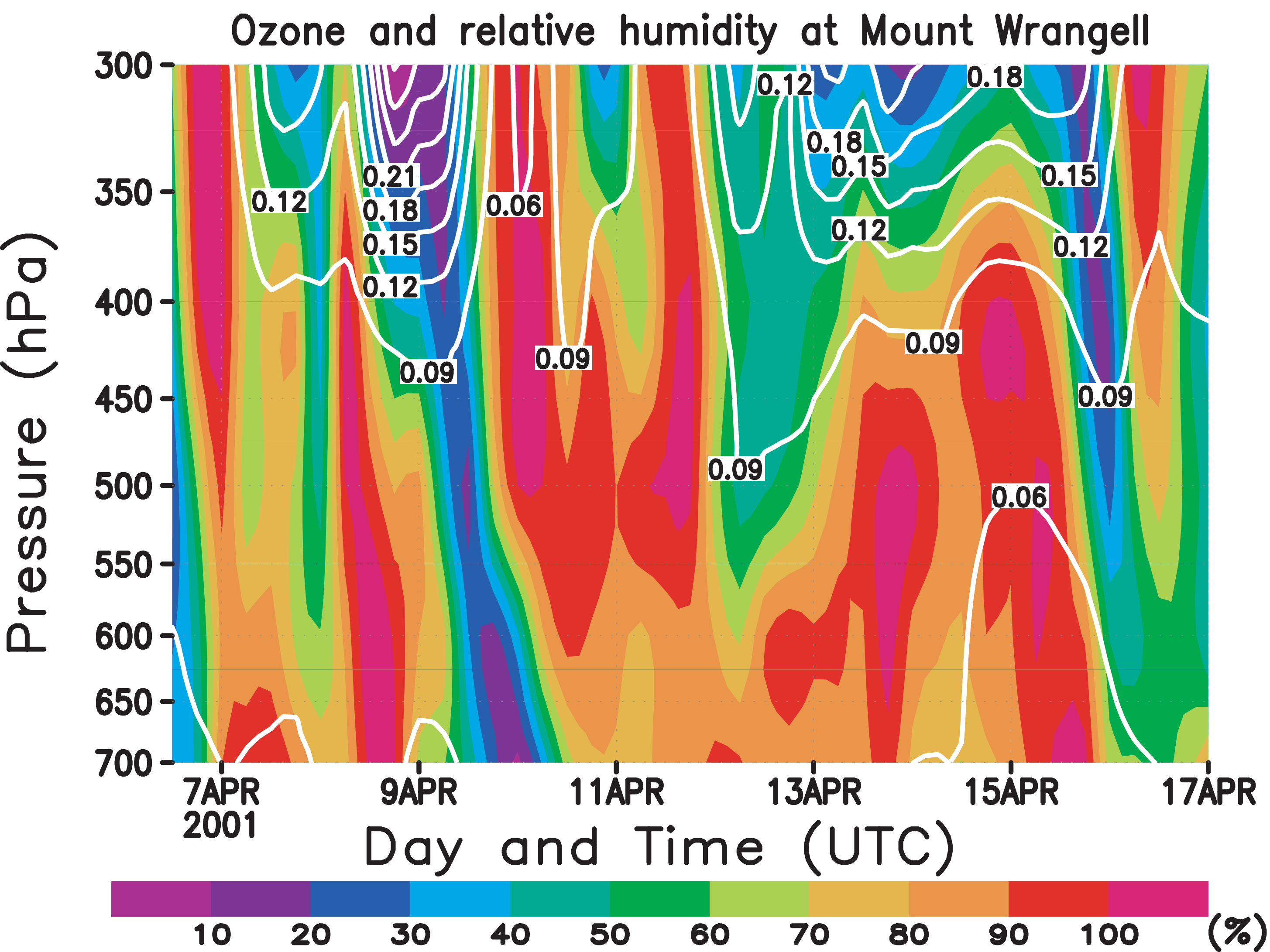

Ozone and relative humidity at Mount Wrangell
Pressure (hPa)
300
350
400
450
500
550
600
650
700
0.12
0.21
0.18
0.15
0.12
0.09
0.06
0.09
0.09
0.12
0.18
0.15
0.12
0.18
0.09
0.06
0.15
0.12
0.09
7APR
2001
9APR
11APR
13APR
15APR
17APR
Day and Time (UTC)
10
20
30
40
50
60
70
80
90
100
(%)

Figure 6

(a)

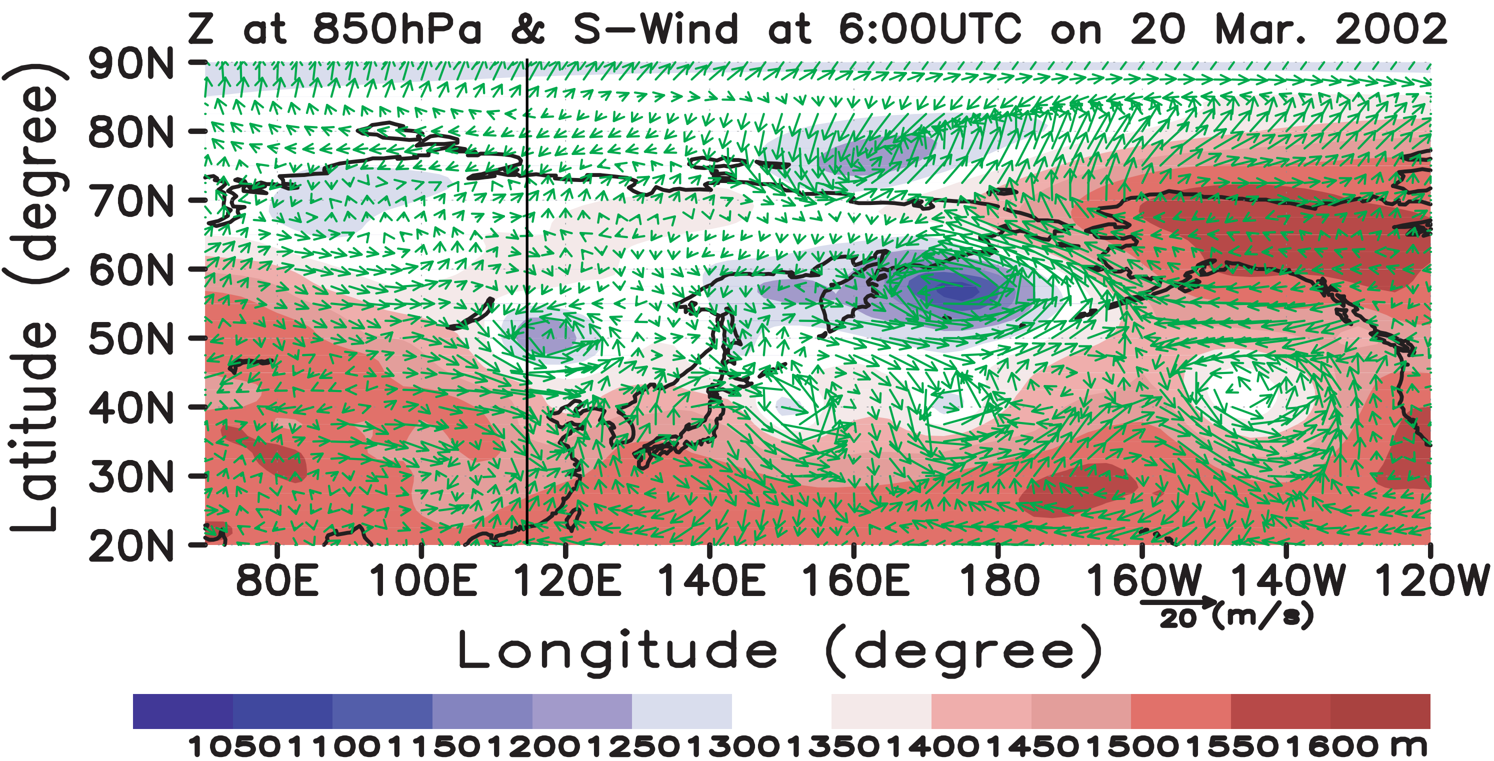
Z at 850hPa & S-Wind at 6:00UTC on 20 Mar. 2002
90N
80N
70N
60N
50N
40N
30N
20N
Latitude (degree)
80E 100E 120E 140E 160E 180 160W 140W 120W
20 (m/s)
Longitude (degree)
1050 1100 1150 1200 1250 1300 1350 1400 1450 1500 1550 1600 m

(b)

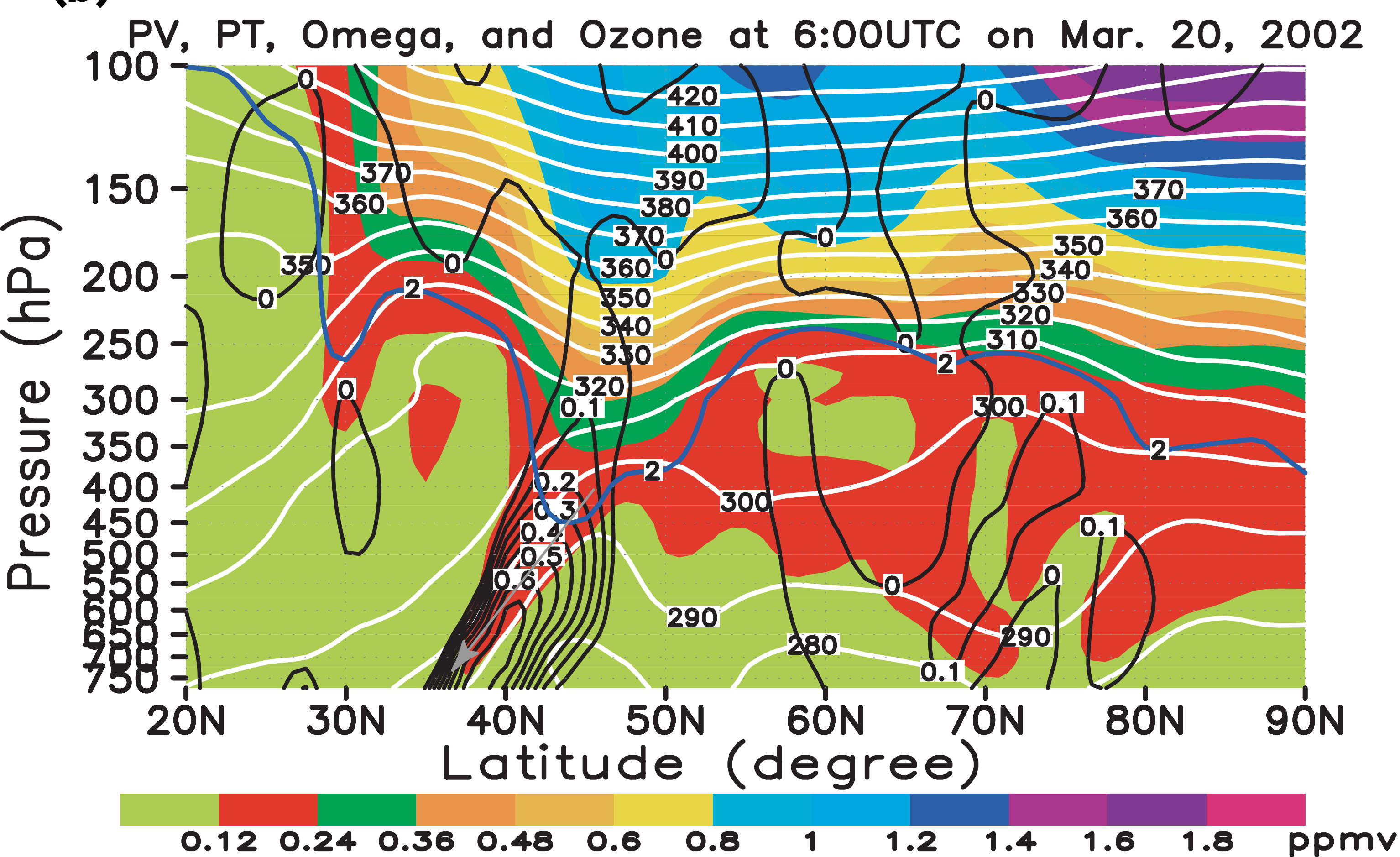
PV, PT, Omega, and Ozone at 6:00UTC on Mar. 20, 2002
100
150
200
250
300
350
400
450
500
550
600
650
700
750
Pressure (hPa)
20N 30N 40N 50N 60N 70N 80N 90N
Latitude (degree)
0.12 0.24 0.36 0.48 0.6 0.8 1 1.2 1.4 1.6 1.8 ppmv

Figure 7
Click here to download high resolution image

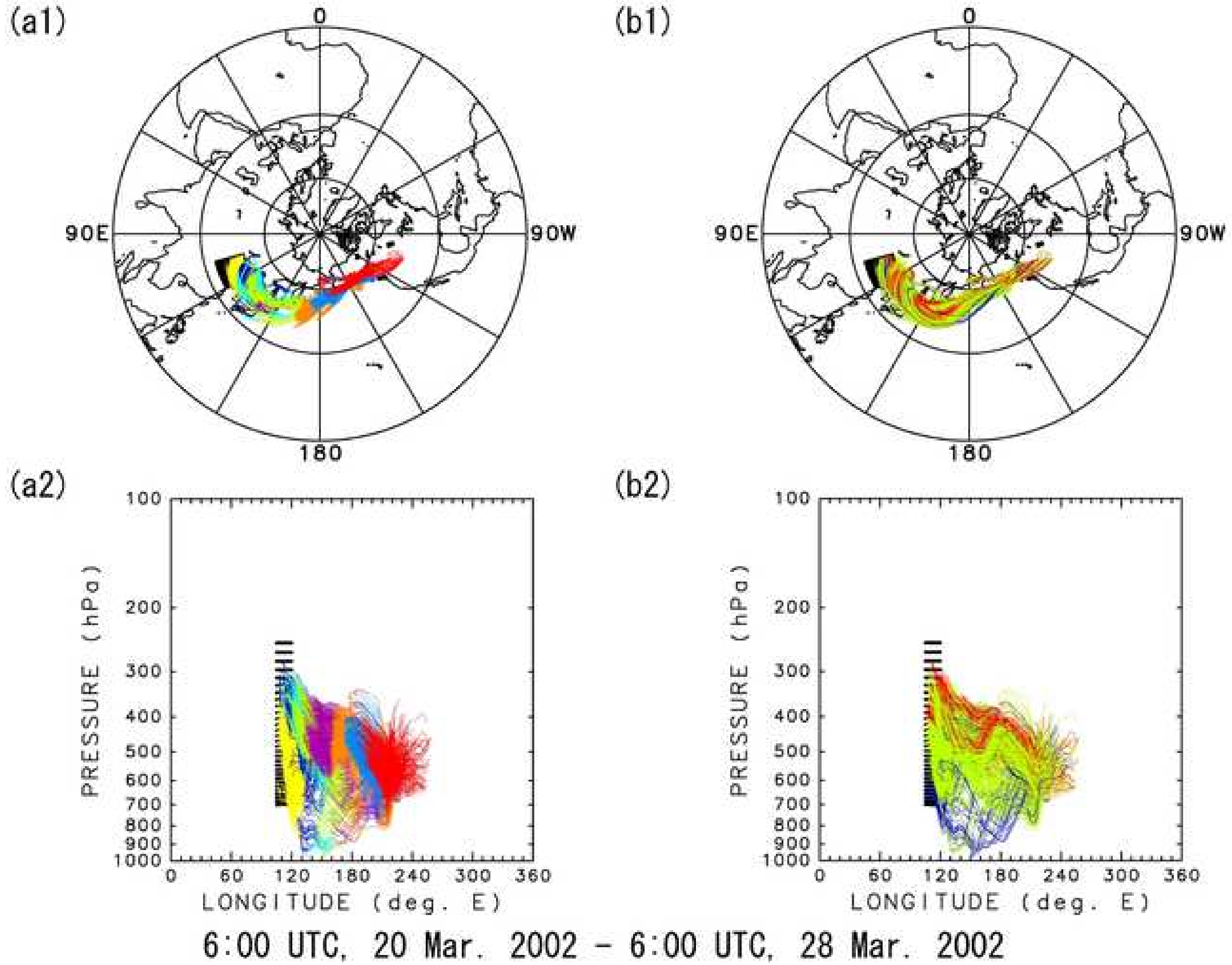

Figure 8

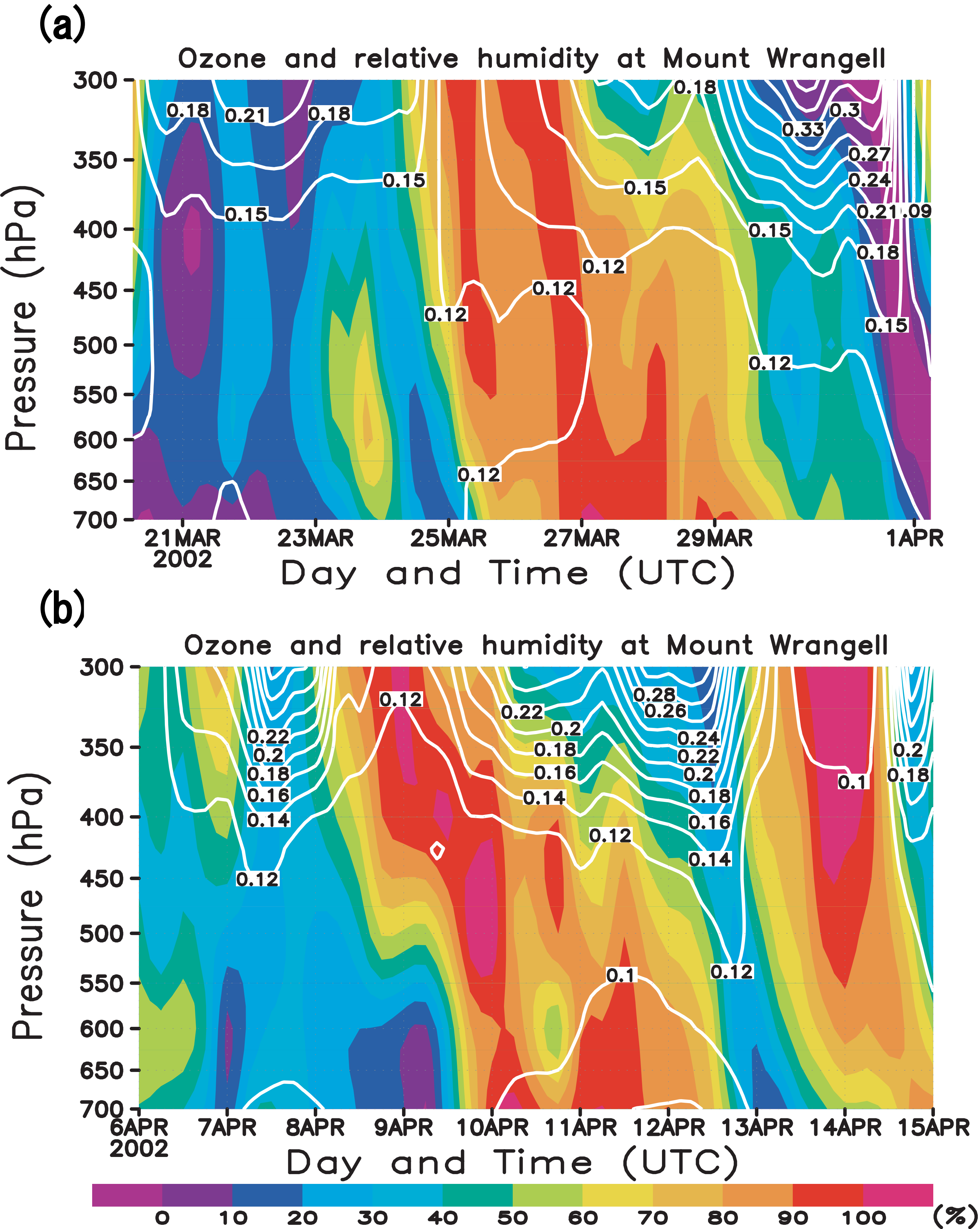
(a)
Ozone and relative humidity at Mount Wrangell
Pressure (hPa)
300
350
400
450
500
550
600
650
700
21MAR 2002
23MAR
25MAR
27MAR
29MAR
1APR
Day and Time (UTC)
(b)
Ozone and relative humidity at Mount Wrangell
Pressure (hPa)
300
350
400
450
500
550
600
650
700
6APR 2002
7APR
8APR
9APR
10APR
11APR
12APR
13APR
14APR
15APR
Day and Time (UTC)
0
10
20
30
40
50
60
70
80
90
100
(%)

Supplementary Material Submission for Atmospheric Environment

Impacts of Asian dust storm associated with the stratosphere-to-troposphere transport in the spring of 2001 and 2002 on dust and tritium variations in Mount Wrangell ice core, Alaska

Teppei J. Yasunari[1] and Koji Yamazaki[2]

[1]Research Institute for Humanity and Nature, Motoyama 457-4, Kamigamo, Kita-ku, Kyoto 603-8047, Japan. (teppei@chikyu.ac.jp)

[2]Graduate School of Environmental Science, Hokkaido University, Kita-10 Nishi-5, Sapporo 060-0810, Japan. (yamazaki@ees.hokudai.ac.jp)

Introduction

The following 11 figures and 1 animation movie of ozone transport at 300 hPa from 12:00UTC on 6 April 2001 to 12:00UTC on 15 April 2001 are submitted as supplementary materials because we would like to reduce the number of figures in main paper and support the connections between STT with and without Asian dust storm. The descriptions in details for the data which we used here were mentioned in the method section 2 in the main paper. Figure numbers were properly mentioned in the main paper with the symbol “S”.

Figure captions for supplementary material

Fig. S1. Meteorological conditions for Asian dust storm at 12:00 UTC on April 6, 2001. (a) Ozone volume mixing ratio (shaded contour; unit: ppmv), 2 PVU tropopause line (blue solid line), and wind (white vector; unit: m s^{-1}) at 300 hPa level. (b) Ozone volume mixing ratio (shaded contour; unit: ppmv), potential temperature (PT; white solid line; unit: K), and vertical p-velocity (omega; black contour; only downward components are plotted; unit: Pa s^{-1}), at the 45°N line (black solid line in Fig. S1a) for the cross-section between longitude and pressure level (<500 hPa). Black solid line in Fig. S1a corresponds to the lines at 45°N. Black arrow in Fig. S1b denotes the place at which STT is occurring.

Figure S2. A case of STT without Asian dust storm. Similar to Fig. S1 but for the STT at 18:00UTC on April 9, 2001. (b) is at the 182.5° E line for the cross section between latitude and pressure level (<700 hPa). Black line in Fig. S2a corresponds to the line at 182.5° E. Black arrow in Fig. S2b denotes the place at which STT is occurring.

Figure S3. Meteorological conditions for Asian dust storm at 6:00 UTC on April 9, 2001. (a) Geopotential height at 850 hPa (shaded contour; unit: m) and surface wind at 10 m (green vector; unit: m s^{-1}). (b) Ozone volume mixing ratio (shaded contour; unit: ppmv), 2 PVU tropopause line (blue solid line), and wind (white vector; unit: m s^{-1}) at 300 hPa level. (c) Ozone volume mixing ratio (shaded contour; unit: ppmv), potential temperature (PT; white solid line; unit: K), and vertical p-velocity (omega; black contour; only downward components are plotted; unit: Pa s^{-1}), at the 45°N line for the cross-section between longitude and pressure level (<600 hPa). (d) As for (c), but for 110°E line. Data grid is interpolated to a finer grid by cubic interpolation. Black and gray lines in

Fig. S3a correspond to the lines at 110°E and 45°N, respectively. Black arrows in Figs. S3c and S3d denote the place at which STT is occurring.

Fig. S4. Similar to Figure 3 but for the Asian dust storm at 6:00 UTC on 9 April 2001.

Figure S5. Similar to Fig. S1 but for the Asian dust storm at 6:00 UTC on March 20, 2002. (b) is at the 42.5°N line for the cross section between longitude and pressure level (<775 hPa). Black line in Fig. S5a corresponds to the lines at 42.5°N. Black arrow in Fig. S5b denotes the place at which STT is occurring.

Figure S6. Similar to Fig. S3 but for the Asian dust storm at 6:00 UTC on 24 March 2002. (c) is at the 52.5°N line for the cross section between longitude and pressure level (<775 hPa). (d) Same as (c), but for at the 110°E line for the cross section between latitude and pressure level (<775 hPa). Black and gray lines in Fig. S6a correspond to the lines at 110°E and 52.5°N, respectively. Black arrows in Figs. S6c and S6d denote the place at which STT is occurring.

Fig. S7. Similar to Figure 3 but for the Asian dust storm at 6:00 UTC on 24 March 2002.

Figure S8. Similar to Fig. S3 but for the Asian dust storm at 0:00 UTC on 6 April 2002. (c) is at the 45°N line for the cross section between longitude and pressure level (<700 hPa). (d) Same as (c), but for at the 110°E line for the cross section between latitude and pressure level (<700 hPa). Black and gray lines in Fig. S8a correspond to the lines at 110°E and 45°N, respectively. Black arrows in Figs. S8c and S8d denote the place at which STT is occurring.

Fig. S9. Similar to Figure 3 but for the Asian dust storm at 0:00 UTC on 6 April 2002.

Figure S10. Similar to Fig. S3 but for the Asian dust storm at 12:00 UTC on 20 April 2002. (c) is at the 47.5°N line for the cross section between longitude and pressure level (<700 hPa). (d) Same as (c), but for at the 115°E line for the cross section between latitude and pressure level (<700 hPa). Black and gray lines in Fig. S10a correspond to the lines at 115°E and 47.5°N, respectively.

Fig. S11. Similar to Figure 3 but for the Asian dust storm at 12:00 UTC on 20 April 2002.

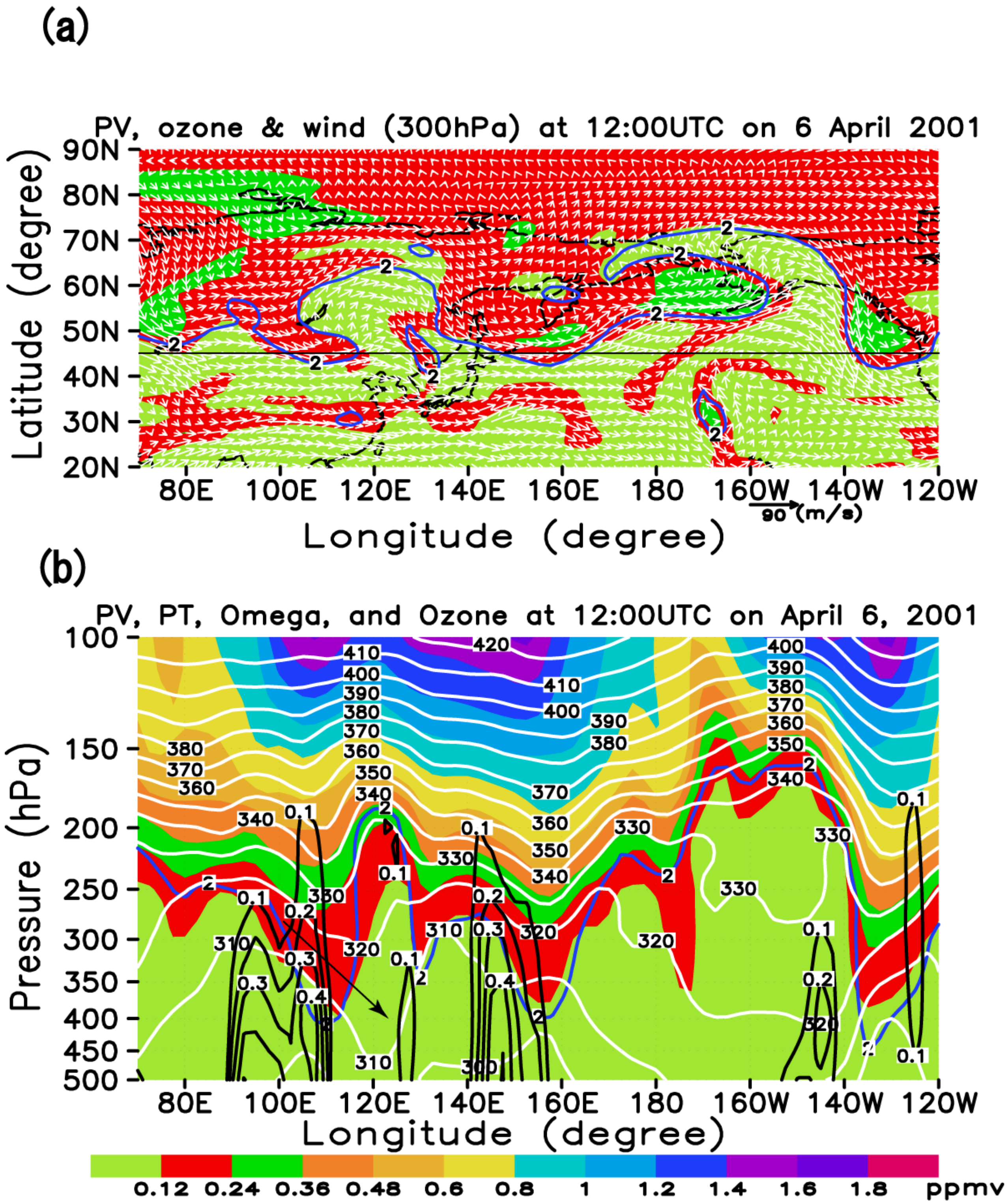
(a)
PV, ozone & wind (300hPa) at 12:00UTC on 6 April 2001
Latitude (degree)
90N
80N
70N
60N
50N
40N
30N
20N
80E 100E 120E 140E 160E 180 160W 140W 120W
90 (m/s)
Longitude (degree)
(b)
PV, PT, Omega, and Ozone at 12:00UTC on April 6, 2001
Pressure (hPa)
100
150
200
250
300
350
400
450
500
80E 100E 120E 140E 160E 180 160W 140W 120W
Longitude (degree)
0.12 0.24 0.36 0.48 0.6 0.8 1 1.2 1.4 1.6 1.8 ppmv

Fig. S1.

(a)

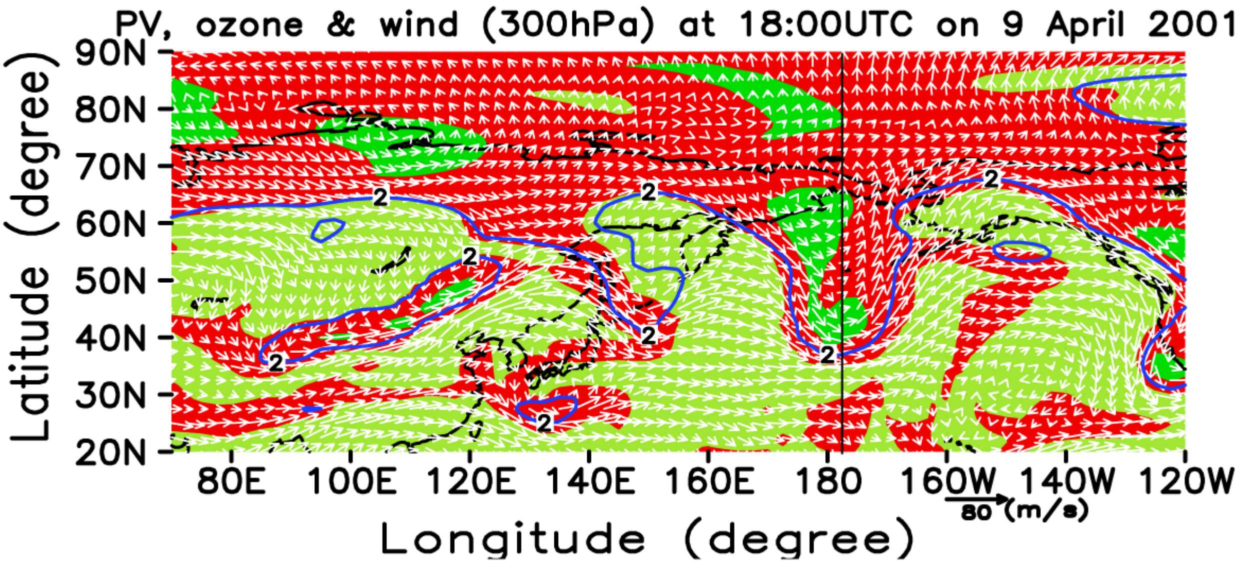
PV, ozone & wind (300hPa) at 18:00UTC on 9 April 2001
Latitude (degree)
Longitude (degree)
80 (m/s)

(b)

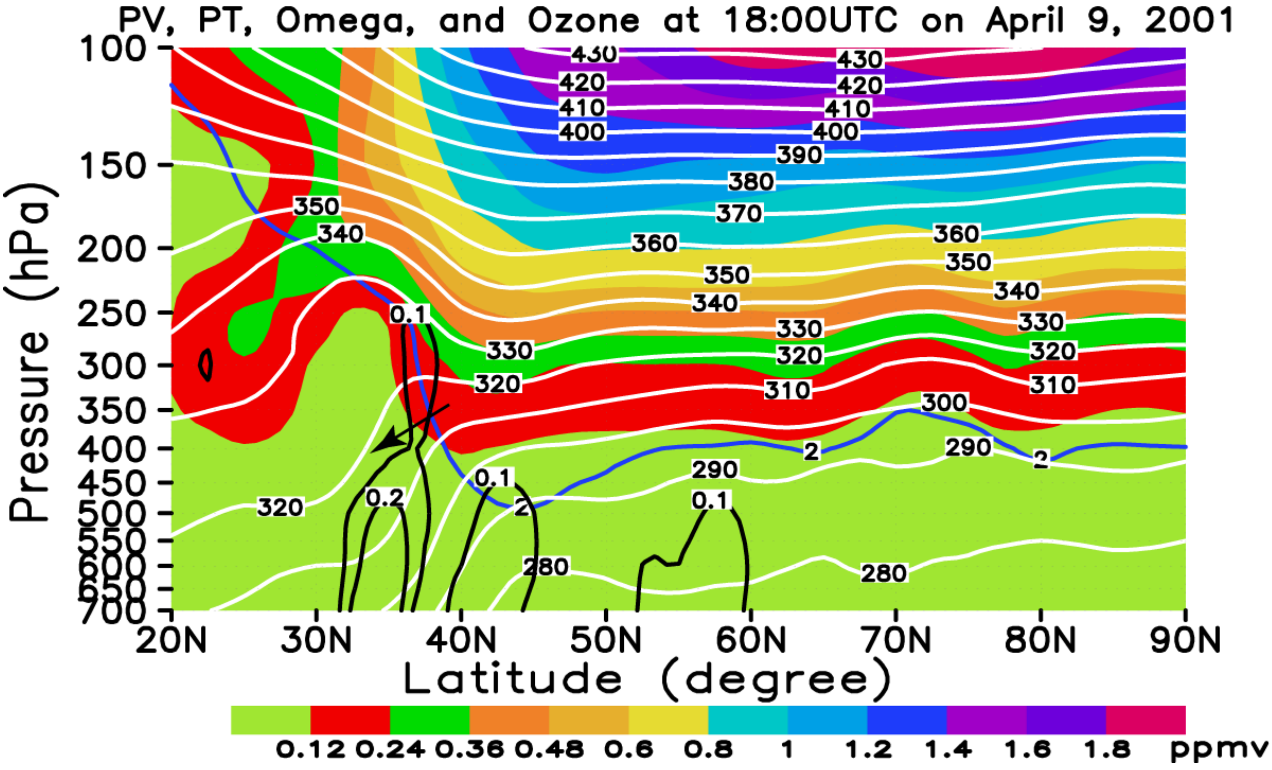
PV, PT, Omega, and Ozone at 18:00UTC on April 9, 2001
Pressure (hPa)
Latitude (degree)
0.12 0.24 0.36 0.48 0.6 0.8 1 1.2 1.4 1.6 1.8 ppmv

Fig. S2.

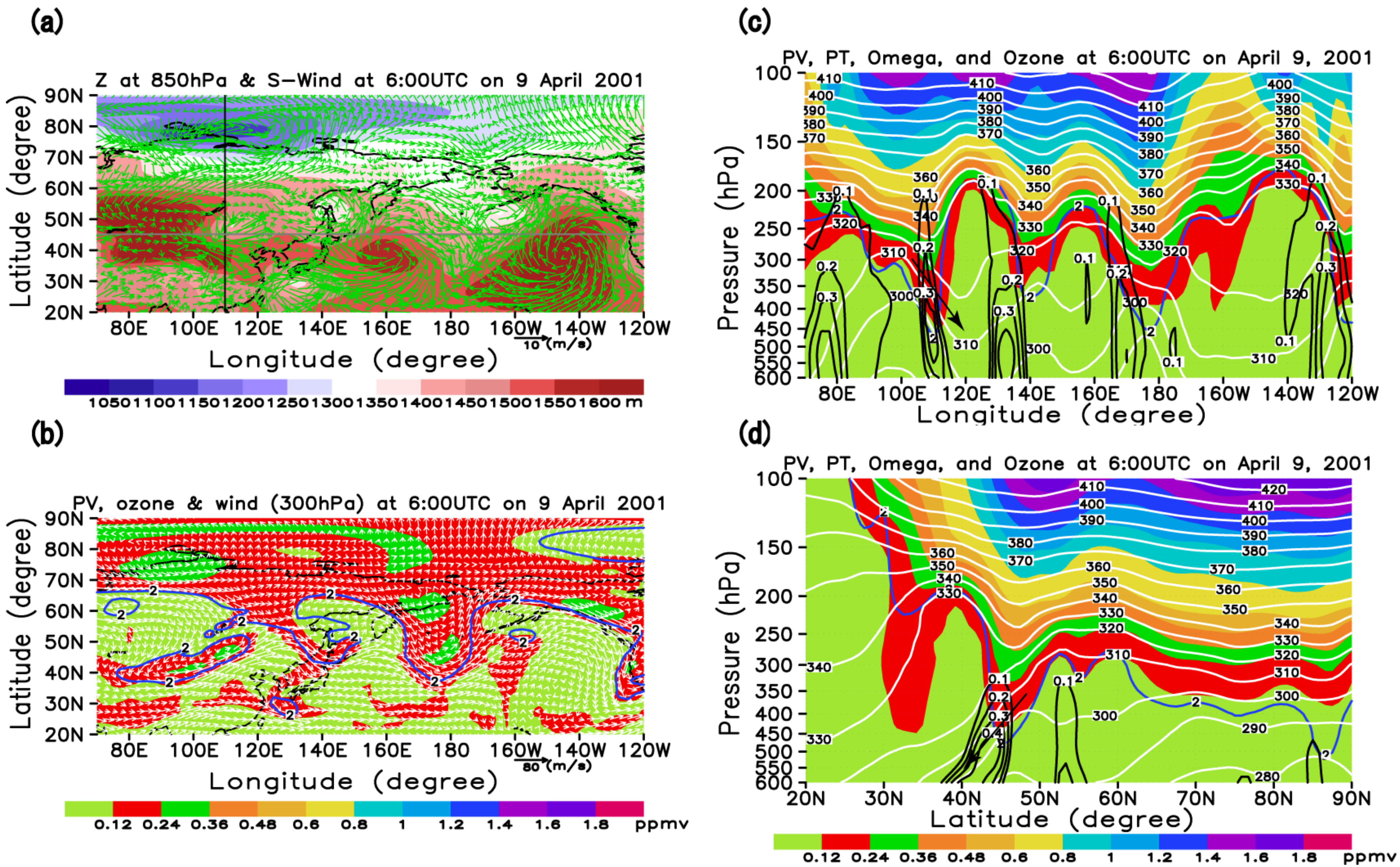
(a)
Z at 850hPa & S-Wind at 6:00UTC on 9 April 2001
Latitude (degree)
Longitude (degree)
10 (m/s)
1050 1100 1150 1200 1250 1300 1350 1400 1450 1500 1550 1600 m
(b)
PV, ozone & wind (300hPa) at 6:00UTC on 9 April 2001
Latitude (degree)
Longitude (degree)
80 (m/s)
0.12 0.24 0.36 0.48 0.6 0.8 1 1.2 1.4 1.6 1.8 ppmv
(c)
PV, PT, Omega, and Ozone at 6:00UTC on April 9, 2001
Pressure (hPa)
Longitude (degree)
(d)
PV, PT, Omega, and Ozone at 6:00UTC on April 9, 2001
Pressure (hPa)
Latitude (degree)
0.12 0.24 0.36 0.48 0.6 0.8 1 1.2 1.4 1.6 1.8 ppmv

Fig. S3.

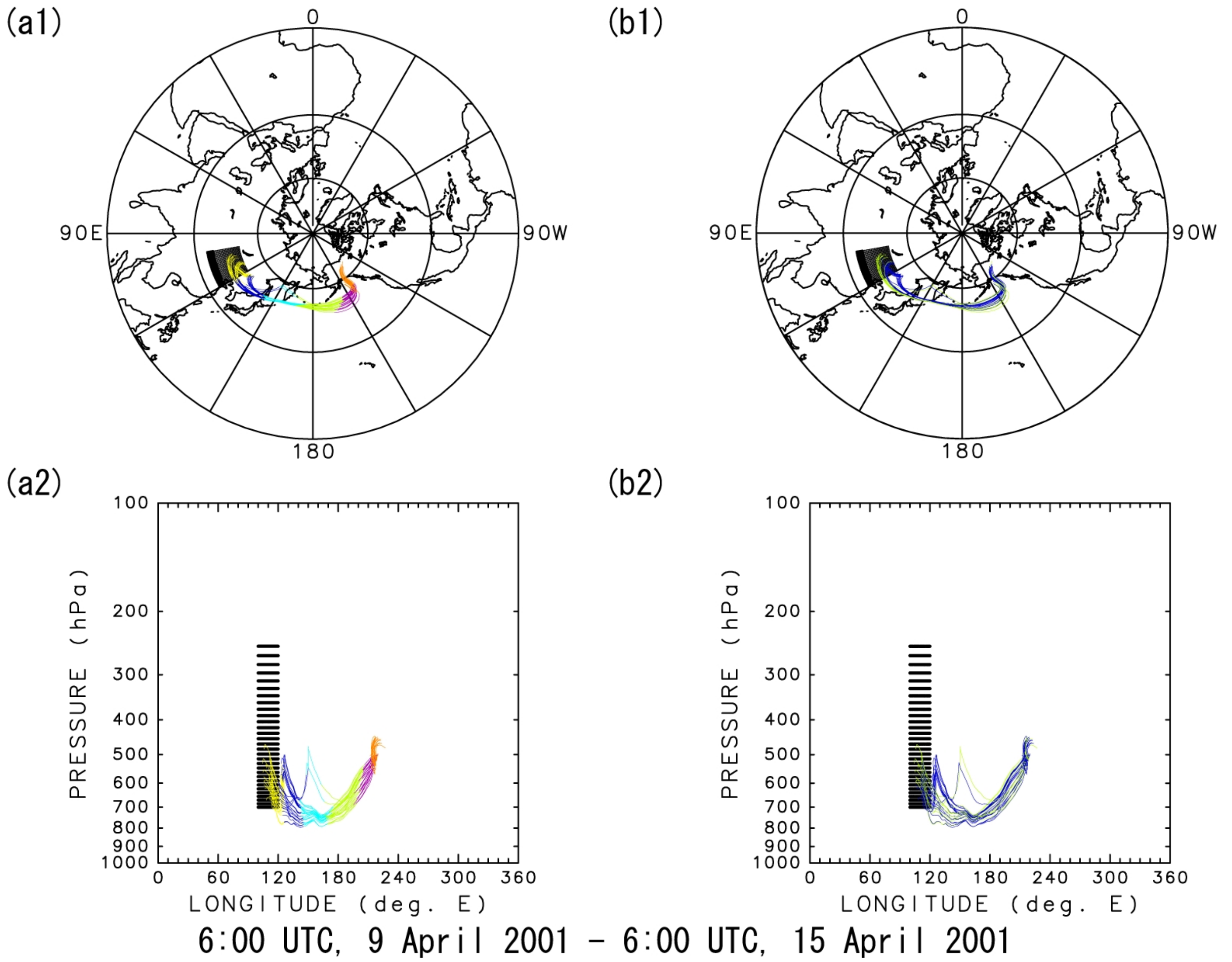
(a1)
(b1)
0
90E
90W
180
(a2)
(b2)
PRESSURE (hPa)
100
200
300
400
500
600
700
800
900
1000
0 60 120 180 240 300 360
LONGITUDE (deg. E)
6:00 UTC, 9 April 2001 - 6:00 UTC, 15 April 2001

Fig. S4.

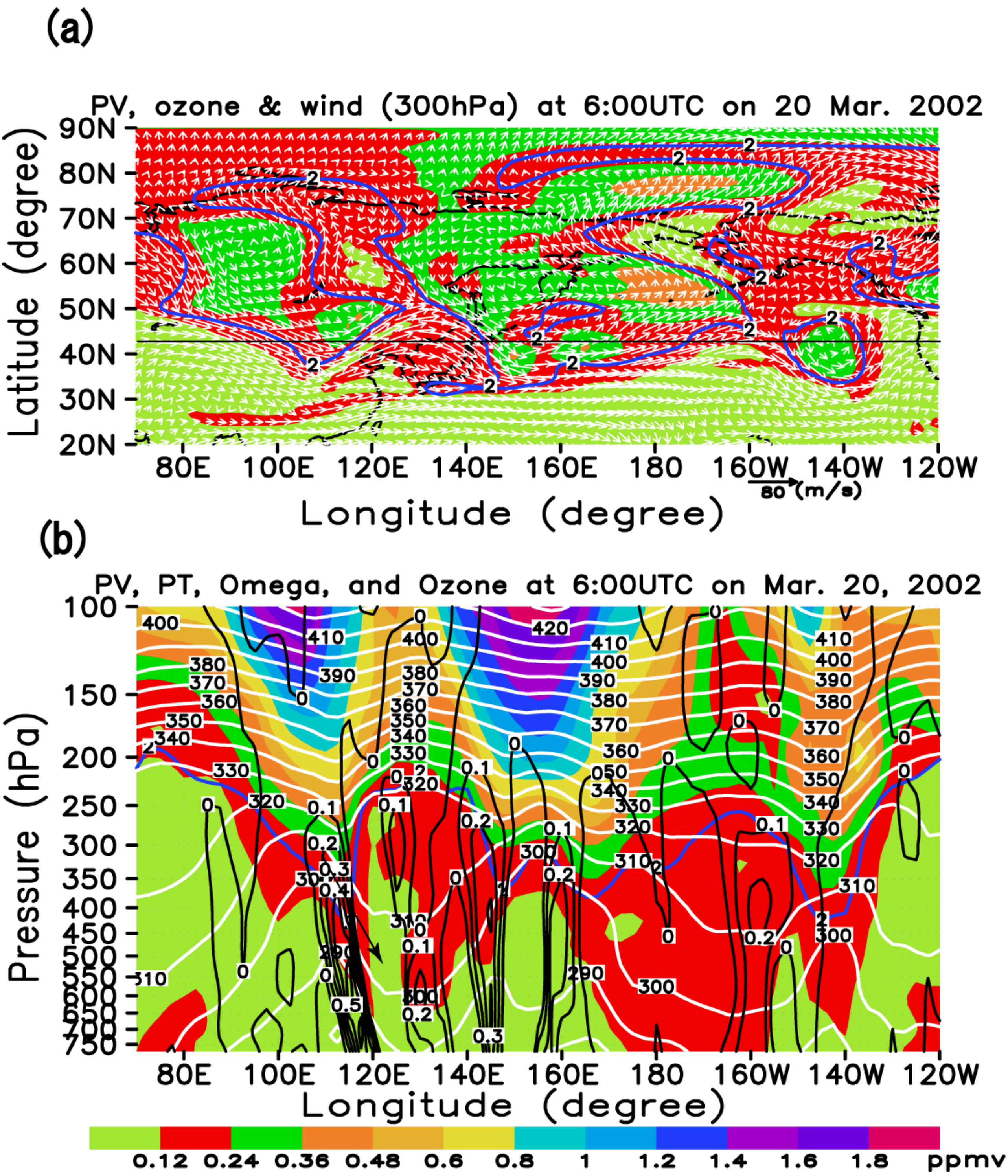
(a)
PV, ozone & wind (300hPa) at 6:00UTC on 20 Mar. 2002
Latitude (degree)
90N
80N
70N
60N
50N
40N
30N
20N
80E 100E 120E 140E 160E 180 160W 140W 120W
80 (m/s)
Longitude (degree)
(b)
PV, PT, Omega, and Ozone at 6:00UTC on Mar. 20, 2002
Pressure (hPa)
100
150
200
250
300
350
400
450
500
550
600
650
700
750
80E 100E 120E 140E 160E 180 160W 140W 120W
Longitude (degree)
0.12 0.24 0.36 0.48 0.6 0.8 1 1.2 1.4 1.6 1.8 ppmv

Fig. S5.

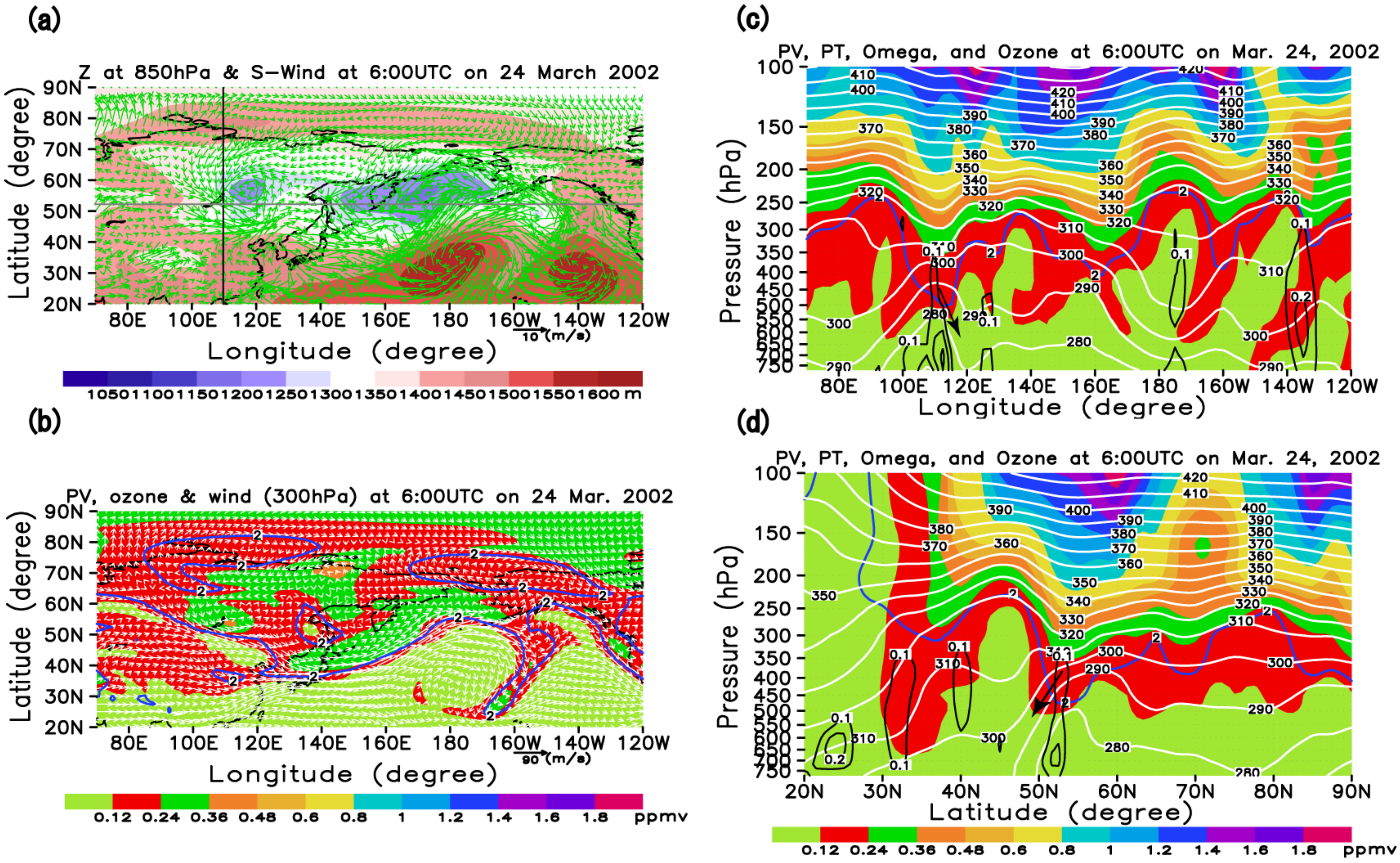

(a)
Z at 850hPa & S-Wind at 6:00UTC on 24 March 2002
Latitude (degree)
Longitude (degree)
10 (m/s)
1050 1100 1150 1200 1250 1300 1350 1400 1450 1500 1550 1600 m
(b)
PV, ozone & wind (300hPa) at 6:00UTC on 24 Mar. 2002
Latitude (degree)
Longitude (degree)
90 (m/s)
0.12 0.24 0.36 0.48 0.6 0.8 1 1.2 1.4 1.6 1.8 ppmv
(c)
PV, PT, Omega, and Ozone at 6:00UTC on Mar. 24, 2002
Pressure (hPa)
Longitude (degree)
(d)
PV, PT, Omega, and Ozone at 6:00UTC on Mar. 24, 2002
Pressure (hPa)
Latitude (degree)
0.12 0.24 0.36 0.48 0.6 0.8 1 1.2 1.4 1.6 1.8 ppmv

Fig. S6.

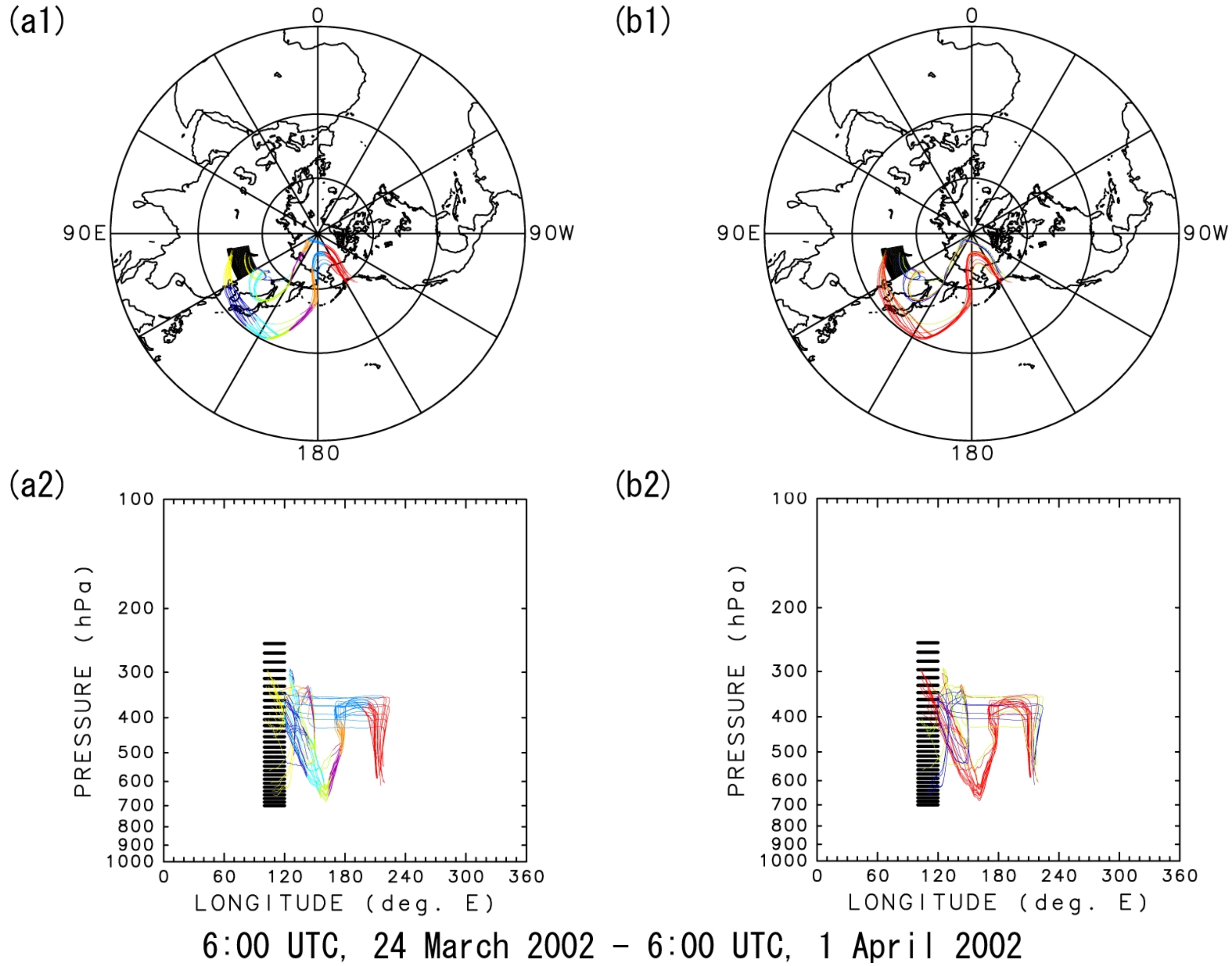
(a1)
0
90E
90W
180
(b1)
0
90E
90W
180
(a2)
100
200
300
400
500
600
700
800
900
1000
PRESSURE (hPa)
0
60
120
180
240
300
360
LONGITUDE (deg. E)
(b2)
100
200
300
400
500
600
700
800
900
1000
PRESSURE (hPa)
0
60
120
180
240
300
360
LONGITUDE (deg. E)
6:00 UTC, 24 March 2002 - 6:00 UTC, 1 April 2002

Fig. S7.

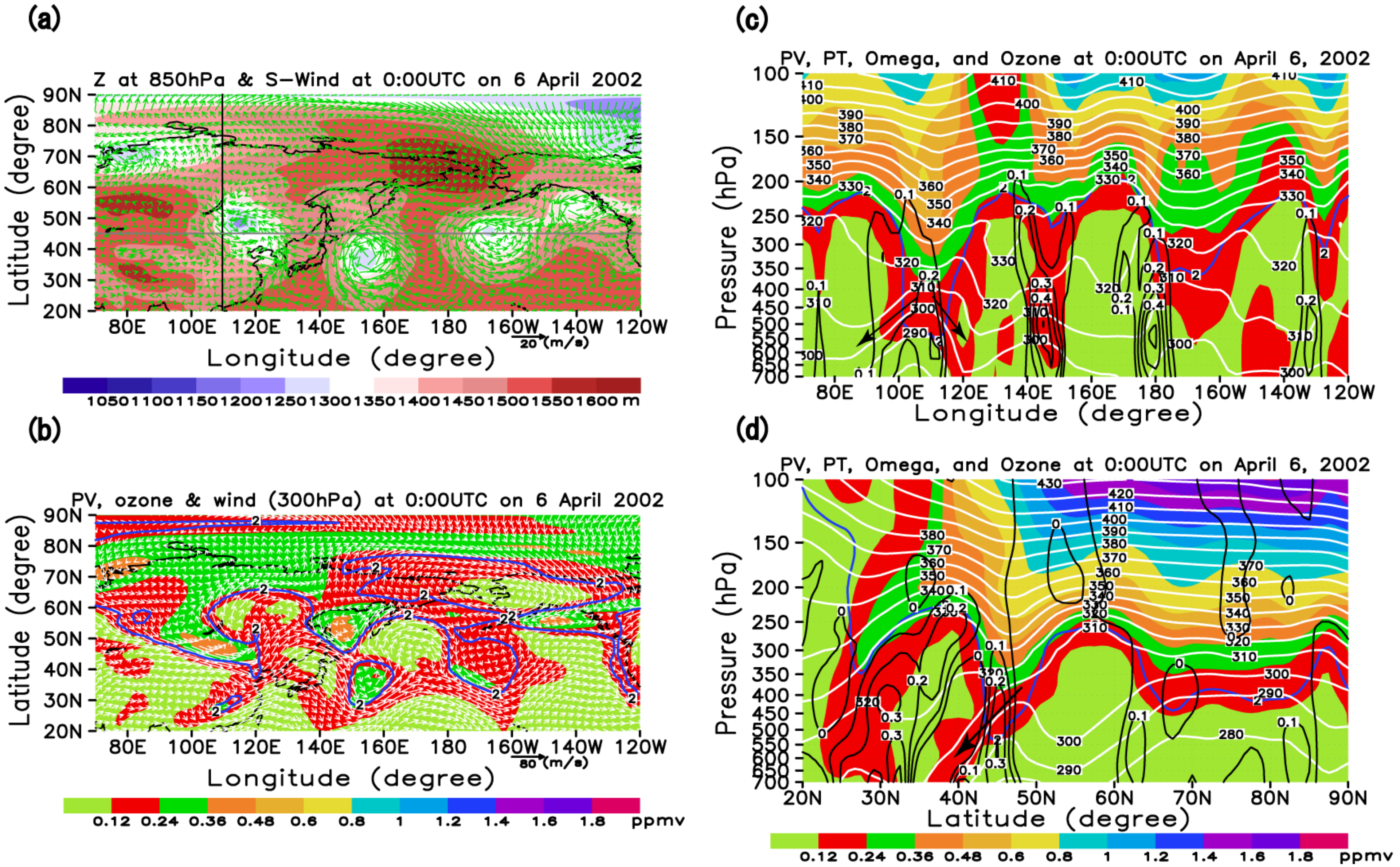
(a)
Z at 850hPa & S-Wind at 0:00UTC on 6 April 2002
Latitude (degree)
Longitude (degree)
20 (m/s)
1050 1100 1150 1200 1250 1300 1350 1400 1450 1500 1550 1600 m
(b)
PV, ozone & wind (300hPa) at 0:00UTC on 6 April 2002
Latitude (degree)
Longitude (degree)
80 (m/s)
0.12 0.24 0.36 0.48 0.6 0.8 1 1.2 1.4 1.6 1.8 ppmv
(c)
PV, PT, Omega, and Ozone at 0:00UTC on April 6, 2002
Pressure (hPa)
Longitude (degree)
(d)
PV, PT, Omega, and Ozone at 0:00UTC on April 6, 2002
Pressure (hPa)
Latitude (degree)
0.12 0.24 0.36 0.48 0.6 0.8 1 1.2 1.4 1.6 1.8 ppmv

Fig. S8

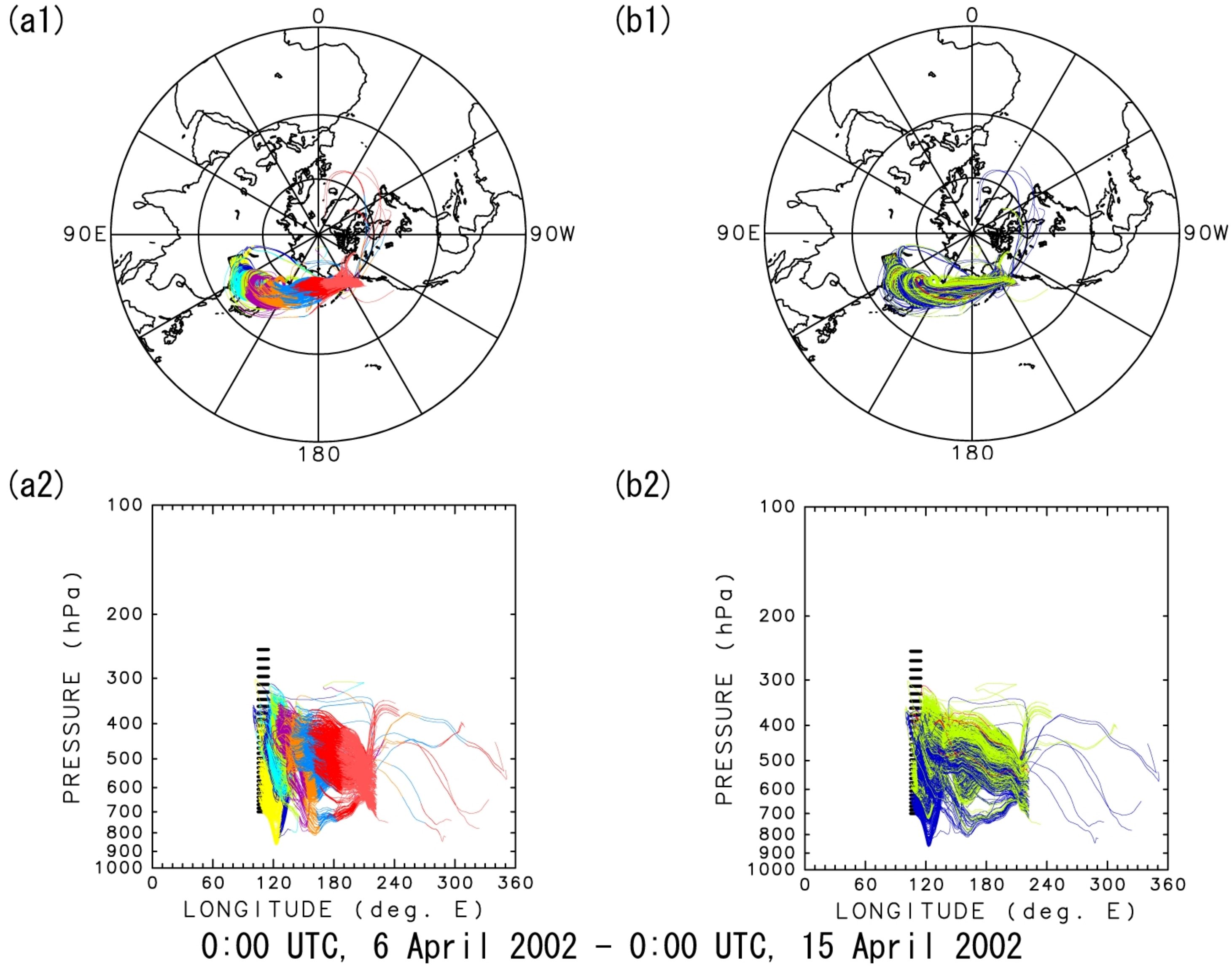

(a1)
0
90E
90W
180
(b1)
0
90E
90W
180
(a2)
PRESSURE (hPa)
100
200
300
400
500
600
700
800
900
1000
0 60 120 180 240 300 360
LONGITUDE (deg. E)
(b2)
PRESSURE (hPa)
100
200
300
400
500
600
700
800
900
1000
0 60 120 180 240 300 360
LONGITUDE (deg. E)
0:00 UTC, 6 April 2002 - 0:00 UTC, 15 April 2002

Fig. S9.

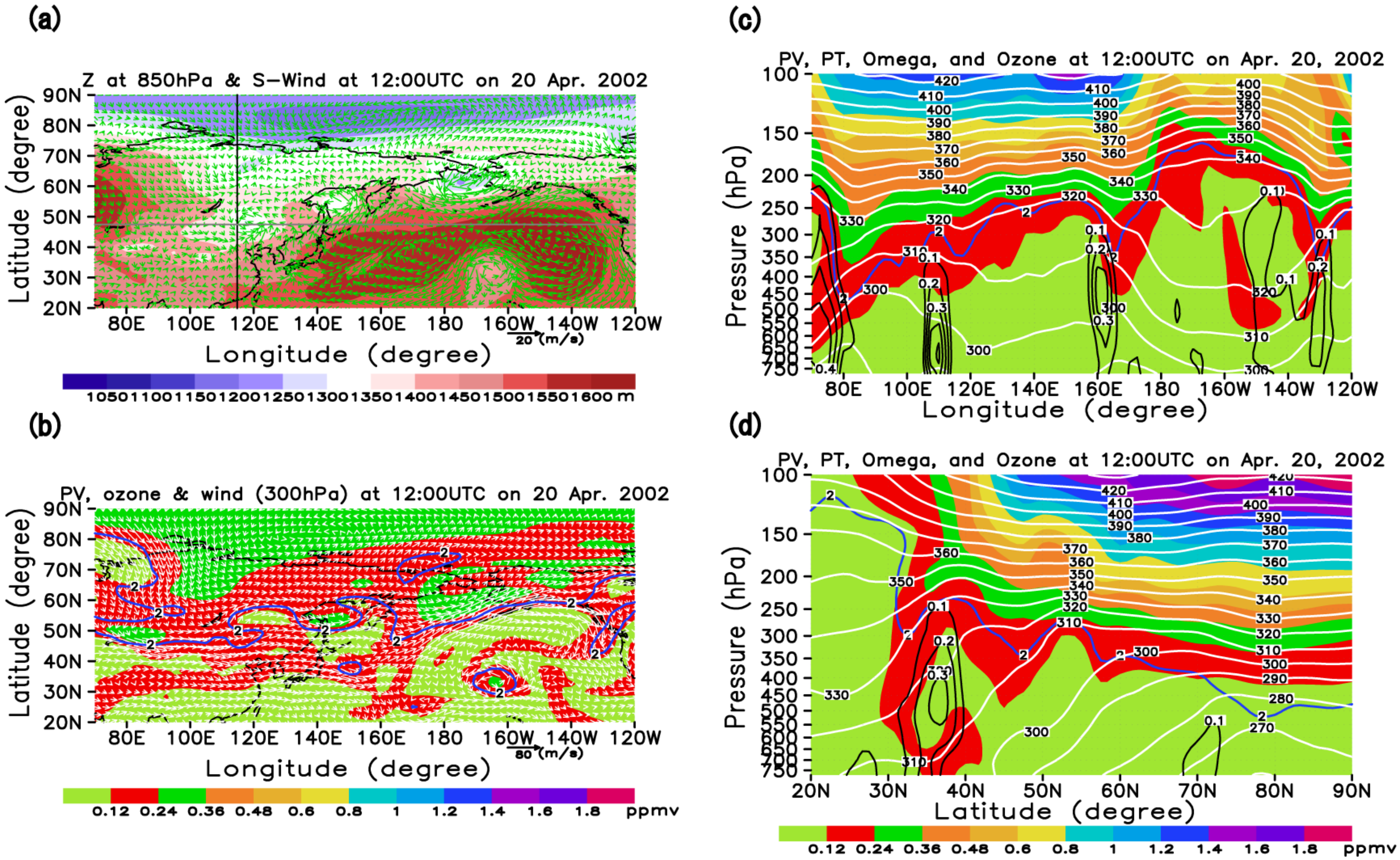

(a)
Z at 850hPa & S−Wind at 12:00UTC on 20 Apr. 2002
90N
80N
70N
60N
50N
40N
30N
20N
Latitude (degree)
80E 100E 120E 140E 160E 180 160W 140W 120W
20 (m/s)
Longitude (degree)
1050 1100 1150 1200 1250 1300 1350 1400 1450 1500 1550 1600 m
(b)
PV, ozone & wind (300hPa) at 12:00UTC on 20 Apr. 2002
90N
80N
70N
60N
50N
40N
30N
20N
Latitude (degree)
80E 100E 120E 140E 160E 180 160W 140W 120W
80 (m/s)
Longitude (degree)
0.12 0.24 0.36 0.48 0.6 0.8 1 1.2 1.4 1.6 1.8 ppmv
(c)
PV, PT, Omega, and Ozone at 12:00UTC on Apr. 20, 2002
100
150
200
250
300
350
400
450
500
550
600
650
700
750
Pressure (hPa)
80E 100E 120E 140E 160E 180 160W 140W 120W
Longitude (degree)
(d)
PV, PT, Omega, and Ozone at 12:00UTC on Apr. 20, 2002
100
150
200
250
300
350
400
450
500
550
600
650
700
750
Pressure (hPa)
20N 30N 40N 50N 60N 70N 80N 90N
Latitude (degree)
0.12 0.24 0.36 0.48 0.6 0.8 1 1.2 1.4 1.6 1.8 ppmv

Fig. S10.

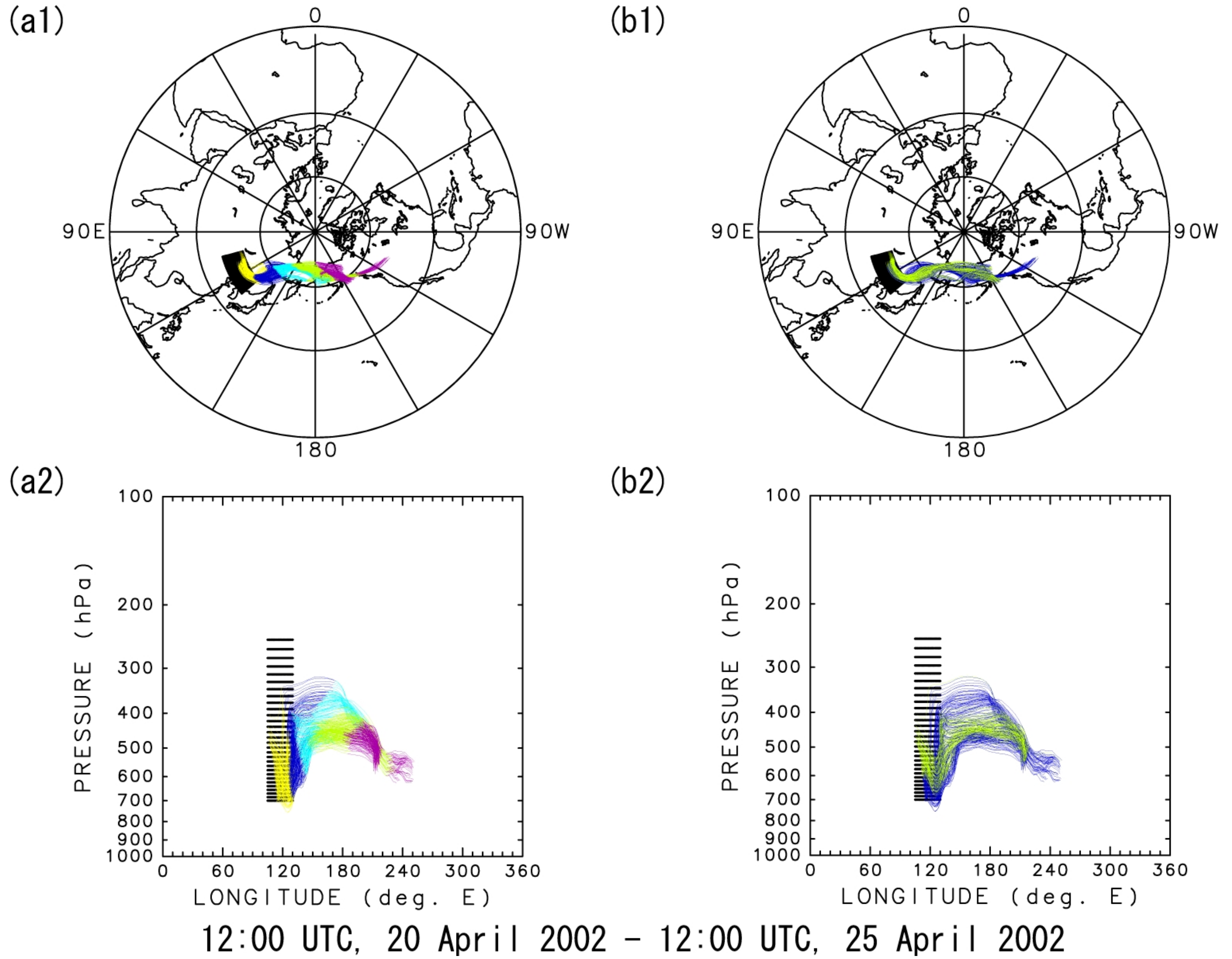
(a1)
0
90E
90W
180
(b1)
0
90E
90W
180
(a2)
PRESSURE (hPa)
100
200
300
400
500
600
700
800
900
1000
0
60
120
180
240
300
360
LONGITUDE (deg. E)
(b2)
PRESSURE (hPa)
100
200
300
400
500
600
700
800
900
1000
0
60
120
180
240
300
360
LONGITUDE (deg. E)
12:00 UTC, 20 April 2002 - 12:00 UTC, 25 April 2002

Fig. S11

Supplementary movie

http://wwwoa.ees.hokudai.ac.jp/people/yamazaki/papers/YasuYama-AE2009-sup1.avi